Electronic Supplementary Information for

Stepwise structural and fluorescent colour conversion in rhodamine analogues based on light and acid stimulations

Masaru Tanioka,§[a,b] Shinichiro Kamino,*§[a,b] Natsumi Koga[a] and Daisuke Sawada*[a,b]

[a.] Graduate School of Medicine, Dentistry and Pharmaceutical Sciences, Okayama University, Okayama-shi, Okayama 700-8530, Japan.
E-mail: skamino@okayama-u.ac.jp; dsawada@okayama-u.ac.jp

[b.] Advanced Elements Chemistry Laboratory, RIKEN-CPR, Hirosawa Wako-shi Saitama 351-0198, Japan.

§ Present Address: Aichi Gakuin University, School of Pharmacy, Kusumoto-cho, Chikusa-ku, Nagoya, 464-8650, Japan.

Table of Contents

1. General Remarks

Materials. Reagents and solvents were commercially available and used as purchased from Tokyo Chemical Industries (Tokyo, Japan), Wako Pure Chemical Industries (Osaka, Japan), and Nacalai Tesque (Kyoto, Japan). All solvents were used without further purification. Flash column chromatography was conducted over silica gel (Merck Silica Gel 60 mesh 70-230). Thin-layer chromatography (TLC) was performed on commercial Merck 60F, 254 silica gel plates, and compounds were visualized with a short-wave UV lamp (λ = 254 nm), by staining with an I_2-SiO_2 mixture, and by heating plates that were dipped in ammonium phosphomolybdate sulfate solution.

Instruments. ^{1}H NMR and ^{13}C NMR spectra were recorded using 600 MHz (Varian UNITY INOVA) spectrometers. Solvents used for NMR measurements were $CDCl_3$ and THF-d_8. Mass spectra were recorded by using G6520 (Agilent Technologies, Ltd.). Light source for photochemical reaction and photometric measurements were xenon lamp (1500 W) coupled to HITACHI F-7100 fluorescence spectrophotometer equipped with a temperature controller unit, and PD2-1012-LED lamp (CCS lnc., Japan).

Absorption and fluorescent emission measurement. UV-vis spectra were recorded using a V-570 spectrophotometer (JASCO Co., Ltd.) at 293 K. Absorption measurements over the spectral range from 250 nm to 700 nm were carried out in quartz cells having an optical path length of 1 cm. Fluorescence emission spectra were collected on a F-7100 fluorescence spectrophotometer (HITACHI High-Technologies Co. Ltd.) at 293 K. To obtain an accurate spectrum, spectrum correction was carried out with rhodamine B concentrated solution and a secondary-standard light source. A cut filter was utilized to eliminate multiple lights, such as secondary light, due to the effects of light scattering. All solvents for spectrophotometry were purchased from Nacalai Tesque (Kyoto, Japan).

2. Figures and tables

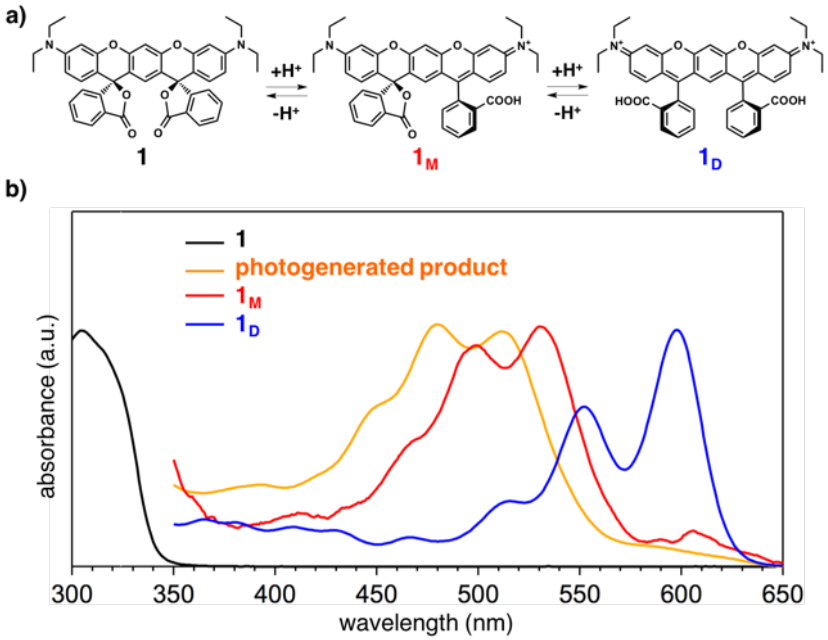

Fig. S1 (a) Protolytic reaction of compound **1**. (b) Absorption spectra of photogenerated product of **1** in $CHCl_3$ after irradiation of UV light, and equilibrium species in various combination of TFA and $CHCl_3$. The black, red, blue and orange curves correspond to the closed, monocationic (**1**$_M$), dicationic (**1**$_D$), and zwitterioninc species of **1**, respectively.

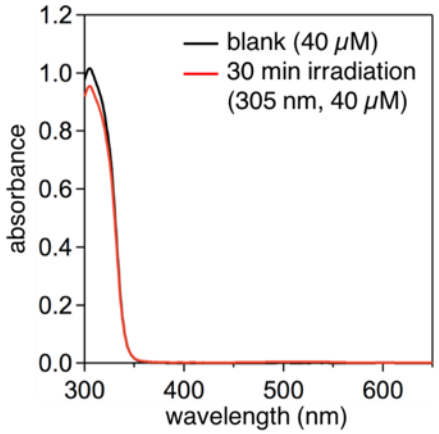

Fig. S2 Absorption spectra of 40 μM of **1** in $CHCl_3$ (black line), and **1** in $CHCl_3$ irradiated with 305 nm UV light for 30 minutes.

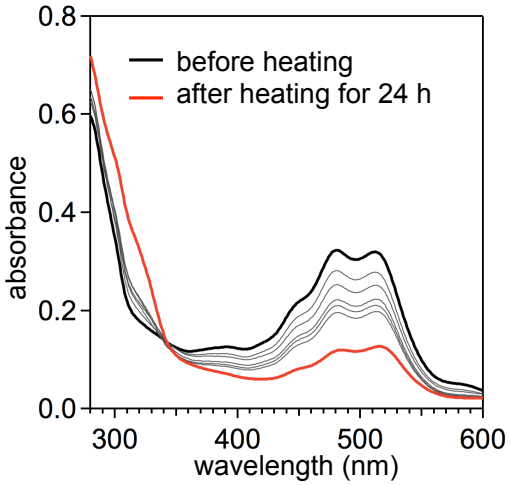

Fig. S3 Absorption spectra of **1z** in degassed $CHCl_3$ upon heating at 313 K.

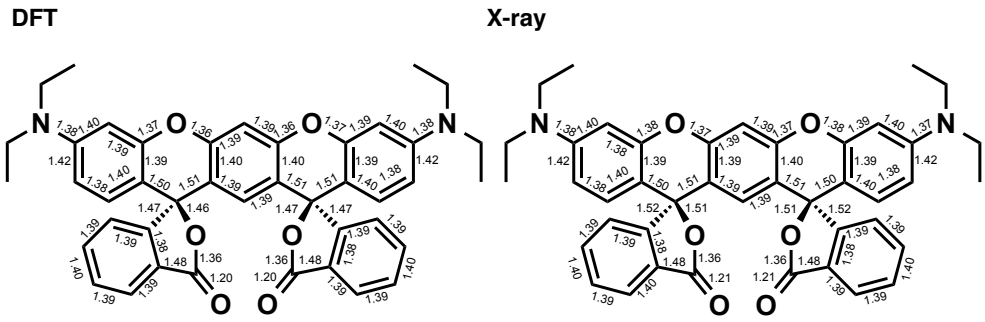

Fig. S4 Comparison of bond lengths (Å) in the DFT-optimized geometry of compound **1** with those in the crystal structure.[1]

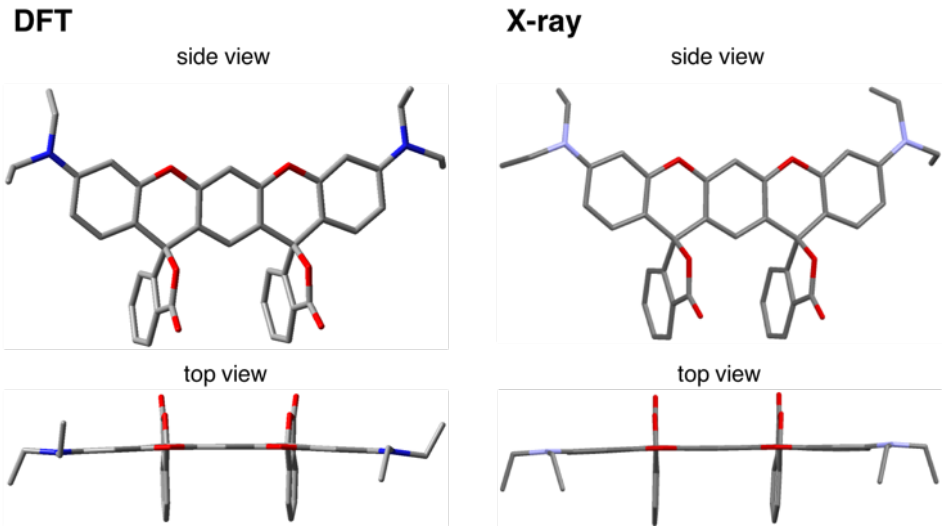

Fig. S5 Comparison the DFT-optimized geometry of compound **1** with the crystal structure.

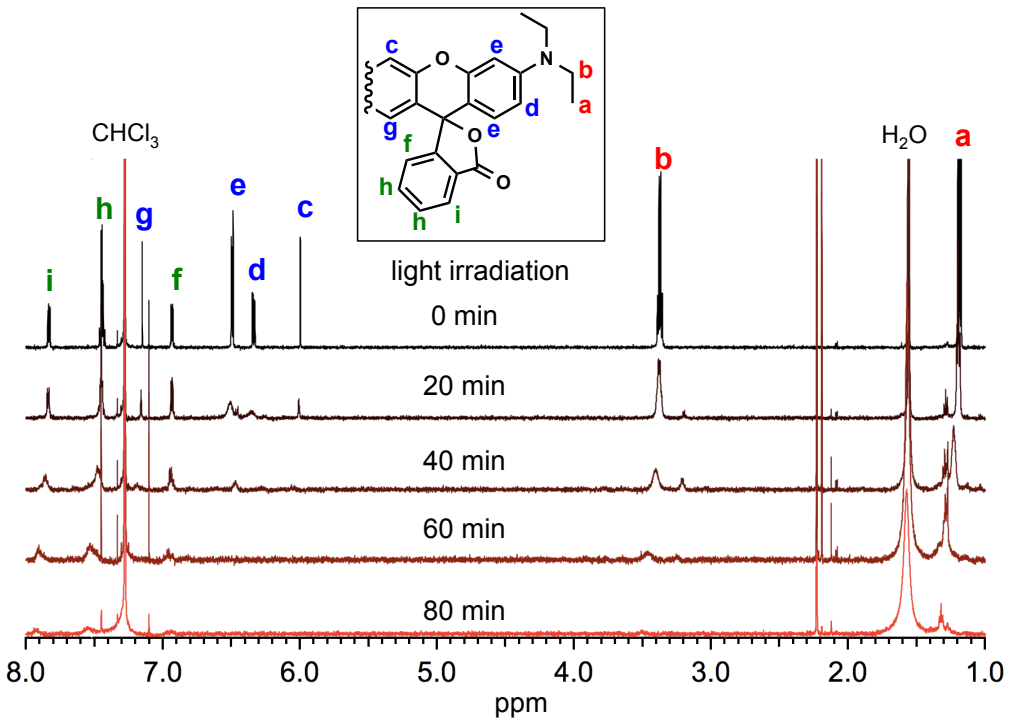

Fig. S6 ^{1}H NMR spectra of **1** in argon-purged $CDCl_3$ upon light irradiation over 0−80 min at 298 K (λ_{irr} = 305 nm, xenon lamp). The inset shows the ^{1}H peaks of **1** in $CDCl_3$. The solution of **1** gave no resonance signals corresponding to the xanthene ^{1}H (H_c−H_g) after 60 min of the irradiation.

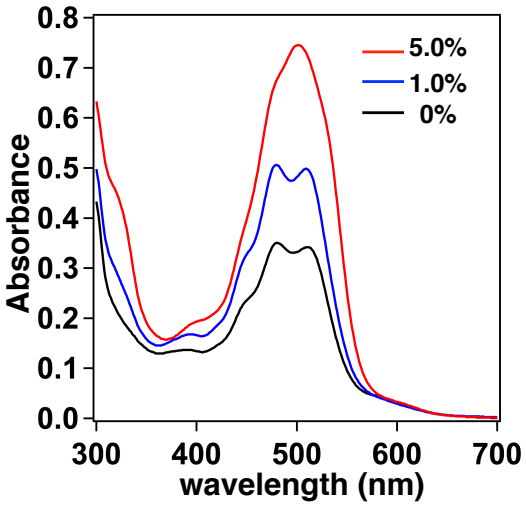

Fig. S7 Absorption spectra of 40 μM of **1** in $CHCl_3$/MeOH solution after UV irradiation for 1 h. The percentages indicate the content of MeOH.

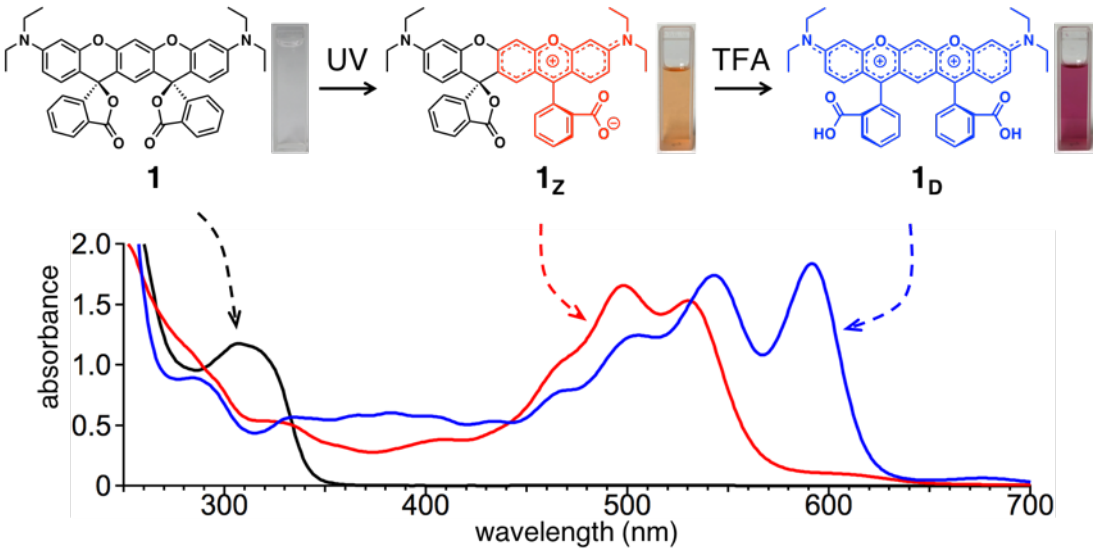

Fig. S8 Schematic illustration and absorption spectra of three states (**1**, $\mathbf{1_Z}$ and $\mathbf{1_D}$) in 1.0% MeOH/$CHCl_3$.

3. Trapping and structural characterization of photogenerated products

3-1. Preparation of cyanoadduct (2)

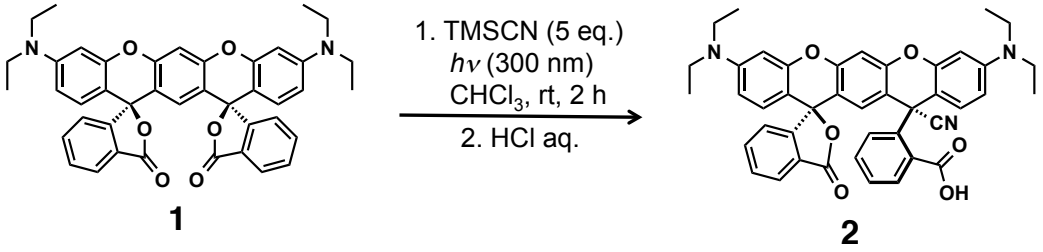

To argon-purged $CHCl_3$ (20 mL) in a dry quartz flask was added compound **1** (13 mg, 2 μM) and TMSCN (9.7 mg, 5 eq.). The reaction mixture was then irradiated with LED lamp (9.5 W, CCS lnc.) peaking at 300 nm for 2 h in the dark condition (The non-irradiated reaction was carried out in the dark condition.). The resulting mixture was acidified with diluted HCl, and allowed to stand at room temperature for 10 min to remove the trimethylsilyl group. The suspension was then extracted with $CHCl_3$ repeatedly. The organic phase was washed with brine, dried over $MgSO_4$ and evaporated to the crude product. This was purified by silica gel column chromatography to obtain the pure product of **2** as white powder. Yield: 2.1 mg (15%).

Compound **2**: ^{1}H NMR (THF-d_8, 600 MHz): δ 7.83-7.89 (m, 2 H), 7.45-7.49 (m, 2 H), 7.24 (dt, 1 H, J = 7.8, 1.2 Hz), 7.11 (dt, 1 H, J = 7.8, 1.2 Hz), 6.97-7.01 (m, 2 H), 6.92-6.95 (m, 1 H), 6.86 (d, 1 H, J = 9 Hz), 6.53 (d, 1 H, J = 9 Hz), 6.43-6.48 (m, 2 H), 6.36 (dd, 1 H, J = 8.4, 2.7 Hz), 6.32 (dd, 1 H, J = 8.7, 2.7 Hz), 6.30 (s, 1 H), 3.28-3.40 (m, 8 H), 1.10-1.20 (m, 12 H). ^{13}C NMR ($CDCl_3$, 150 MHz): δ 172.63, 169.76, 153.52, 152.72, 152.23, 151.89, 151.57, 149.70, 149.47, 147.89, 134.54, 132.99, 131.52, 130.66, 130.54, 129.66, 129.55, 128.96, 127.73, 127.63, 125.94, 124.85, 123.87, 122.03, 115.14, 111.25, 108.46, 108.34, 105.49, 103.71, 98.92, 97.87, 84.69, 44.59, 44.49, 12.74, 12.70, 12.62. HRMS (ESI) calcd for $C_{43}H_{38}N_3O_6$ $[M]^+$: 692.2760, Found 692.2755. IR (KBr) cm^{-1}: 2972, 2854, 1767, 1616.

3-2. Preparation of isopropyl cyano radical adduct (3)

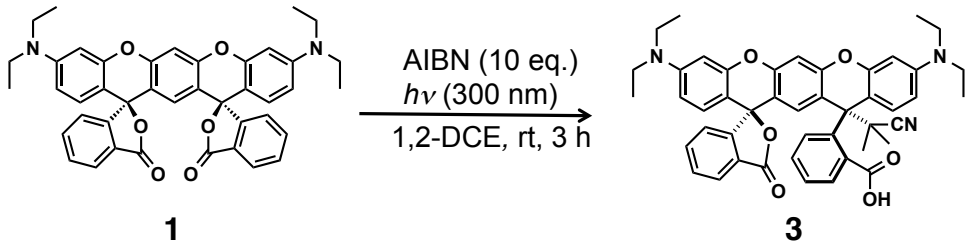

1 **3**

To argon-purged 1,2-DCE (10 ml) in a dry quartz flask was added compound **1** (66 mg, 100 μmol) and AIBN (164 mg, 10 eq.). The resulting mixture was irradiated with LED lamp (9.5 W, CCS lnc.) peaking at 300 nm for 3 h in the dark condition (The non-irradiated reaction was heated to 70℃ in the dark condition.). The reaction mixture was evaporated to give the crude product. This was purified by preparative silica gel column chromatography to obtain the pure product of **3** as white powder. Yield: 8.1 mg (11%).
Compound 3: ^{1}H NMR (THF-d_8, 600 MHz): δ 7.83 (d, 1 H, J = 7.2 Hz), 7.65 (dd, 1 H, J = 7.8, 1.2 Hz), 7.50 (t, 2 H, J = 7.2 Hz), 7.43 (dt, 2 H, J = 7.2, 1.0 Hz), 7.24 (t, 1 H, J = 7.5 Hz), 7.12 (dt, 1 H, J = 7.5, 2.4 Hz), 7.01 (dt, 1 H, J = 7.5, 1 Hz), 6.82-6.92 (m, 4 H), 6.73 (d, 1 H, J = 8.4 Hz), 6.58 (s, 1 H), 6. 49 (d, 1 H, J = 2.4 Hz), 6.47 (d, 1 H, J = 9.6 Hz), 6.41 (d, 1 H, J = 1.8 Hz), 6.35 (dd, 2 H, J = 8.4, 2.4 Hz), 6.28-6.32 (m, 2 H), 3.30-3.42 (m, 8 H), 1.40 (s, 6 H), 1.10-1.17 (m, 12 H). ^{13}C NMR (THF-d_8, 150 MHz): δ 169.40, 168.90, 154.12, 153.50, 153.28, 152.79, 152.67, 152.15, 150.36, 150.03, 148.74, 138.13, 132.49, 131.83, 131.16, 130.87, 130.45, 130.14, 129.97, 129.58, 128.82, 128.67, 126.10, 125.90, 124.85, 124.66, 123.95, 116.55, 112.00, 109.10, 108.91, 106.88, 103.78, 99.25, 98.42, 83.67, 68.21, 44.07, 44.98, 44.83, 37.81, 35.10, 30.73, 26.37, 21.39, 12.96, 12.81. LRMS (FAB$^+$) Found 735. IR (KBr) cm^{-1}: 2972, 1765, 1618.

3-3. Preparation of stylene adducts (4 and 5)

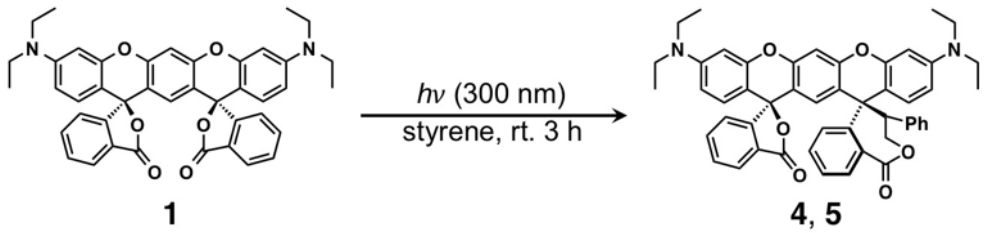

1 **4, 5**

The procedure for the synthesis of compounds **4** and **5** is shown in Scheme 1. A solution of compound **1** (132 mg, 1.5 mmol), and degassed styrene (50 ml) were added into a dry and argon-purged quartz flask. The resulting mixture was then irradiated with LED lamp (9.5 W, CCS lnc.) peaking at 300 nm for 3 h in the dark condition. The reaction mixture was evaporated to give the crude product. This was purified by preparative silica gel column chromatography to obtain the pure product of **4** and **5** as pink powder. Compounds **4** and **5** were identified by ^{1}H-^{1}H COSY, HSQC and HMBC spectra.

Compound **4**: Yield: 7.8 mg (5.1 %). ^{1}H NMR ($CDCl_3$, 600 MHz): δ 7.82-7.87 (m, 2 H), 7.43-7.49 (m, 2 H), 7.12-7.17 (m, 2 H), 7.00-7.05 (m, 1 H), 6.94-7.00 (m, 3 H), 6.87 (dd, 1 H, *J* = 8.1, 0.9 Hz), 6.57 (d, 1 H, *J* = 9.0 Hz), 6.56 (s, 1 H), 6.50 (d, 1 H, *J* = 9.0 Hz), 6.46 (d, 1 H, *J* = 8.4 Hz), 6.36 (dd, 1 H, *J* = 9.3, 2.7 Hz), 6.31 (dd, 1 H, *J* = 9.0, 2.4 Hz), 6.13 (s, 1 H), 5.98-6.04 (m, 3 H), 4.71 (dd, 1 H, *J* = 11.4, 7.2 Hz), 4.26 (d, 1 H, *J* = 12.0 Hz), 3.57 (d, 1 H, *J* = 7.2 Hz), 3.22-3.42 (m, 8 H), 1.18 (t, 6 H, *J* = 6.9 Hz), 1.13 (t, 6 H, *J* = 12.0 Hz). ^{13}C NMR ($CDCl_3$, 150 MHz): δ 170.51, 169.59, 153.44, 153.07, 153.02, 151.62, 151.46, 149.78, 148.03, 146.32, 138.83, 135.23, 134.55, 132.89, 131.36, 131.02, 129.77, 129.50, 129.34, 129.21, 129.03, 128.9, 128.80, 128.50, 128.42, 127.40, 127.02, 126.80, 124.86, 123.89, 123.64, 115.03, 114.75, 108.65, 108.60, 104.68, 103.11, 97.75, 97.40, 68.22, 60.43, 54.38, 44.61, 44.49, 12.62, 12.56. HRMS (ESI) calcd for $C_{50}H_{45}N_2O_6$ $[M]^+$: 769.3272, Found 769.3266. IR (KBr) cm^{-1}: 2970, 2872, 1765, 1616.

Compound **5**: Yield: 3.4 mg (2.2 %). ^{1}H NMR ($CDCl_3$, 600 MHz): δ 7.94 (d, 1 H, *J* = 9.0 Hz), 7.90 (dd, 1 H, *J* = 8.4, 1.8 Hz), 7.48-7.53 (m, 1 H), 7.35 (dt, 1 H, *J* = 7.5, 1.2 Hz), 7.11-7.21 (m, 3 H), 6.92-7.02 (m, 3 H), 6.76 (d, 1 H, *J* = 7.8 Hz), 6.71 (d, 1 H, *J* = 9.0 Hz), 6.61 (s, 1 H), 6.52 (d, 1 H, *J* = 9.0 Hz), 6.44 (d, 1 H, *J* = 1.8 Hz), 6.35 (dd, 1 H, *J* = 8.7, 2.7 Hz), 6.32 (dd, 1 H, *J* = 9.0, 2.4 Hz), 6.04 (d, 2 H, *J* = 7.2 Hz), 6.01 (d, 1 H, *J* = 2.4 Hz), 5.85 (s, 1 H), 5.07 (dd, 1 H, *J* = 6.6, 6.0 Hz), 4.23 (d, 1 H, *J* = 12.0 Hz), 3.43 (d, 1 H, *J* = 6.6 Hz), 3.23-3.41 (m, 8 H), 1.08-1.23 (m, 12 H). ^{13}C NMR ($CDCl_3$, 150 MHz): δ 169.23, 168.99, 153.59, 153.27, 152.06, 151.73, 151.64, 149.73, 148.32, 147.20, 138.77, 135.59, 134,18, 133.38, 131.59, 130.94, 130.37, 129.50, 129.28, 129.00, 128.86, 127.67, 127.32, 126.98, 126.75, 126.47, 125.17, 123.44, 116.18, 112.20, 108.34, 107.74, 105.47, 102.92, 98.11, 97.85, 68.42, 60.38, 54.77, 44.62, 44.62, 44.55, 44.1, 12.61, 12.58, 12.54. HRMS (ESI) calcd for $C_{50}H_{45}N_2O_6$ $[M]^+$: 769.3272, Found 769.3249. IR (KBr) cm^{-1}: 2970, 1766, 1614.

4. Calculation of the excited state dipole moment

In previous report, it was founded that compound **1** exhibited solvatochromic fluorescence. Therefore, the determination of excited state dipole moment (μ_e) of **1** through solvatofluorochromic shifts have been carried out by plotting of Lippert-Mataga and Bilot-Kawski equations, and Reichardt's E_T^N solvent polarity parameter.

Lippert-Mataga equation

$$\nu_{abs} - \nu_{fl} = \frac{2(\mu_e - \mu_g)^2}{hca^3}\left(\frac{\varepsilon - 1}{2\varepsilon + 1} - \frac{n^2 - 1}{2n^2 + 1}\right) + \text{constant} \qquad \text{(Eq. 1)}$$

$$\Delta f = \frac{(\varepsilon - 1)}{(2\varepsilon + 1)} - \frac{(n^2 - 1)}{(2n^2 + 1)} \qquad \text{(Eq. 2)}$$

In the equations of Eq. 1 and Eq. 2, ν_{abs} and ν_{fl} are the wavenumber of the absorption and fluorescence emission; μ_e and μ_g are the excited and ground state dipole moments, respectively; c is the velocity of light; h is Planck's constant; a is the radius of the cavity in which chromophore resides; ε and n are the dielectric constant and the refractive index, respectively of the organic solvent; Δf is the orientation polarizability function. The a calculated from the absolute density of compound **1** was 5.98 Å.

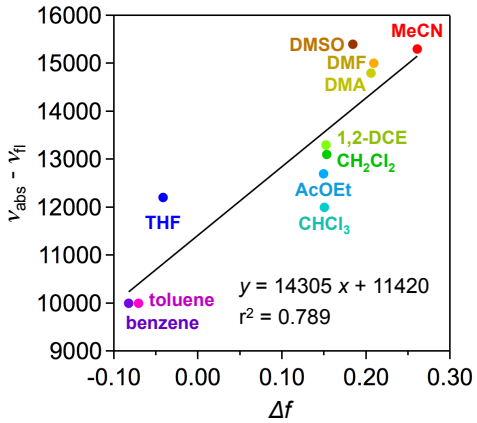

Fig. S9 Lippert-Mataga plots. Stokes shifts ($\nu_{abs} - \nu_{fl}$) *vs* orientation polarizability function (Δf) for **1**. Only aprotic solvents were used.

Bilot-Kawski equation

$$\nu_{abs} - \nu_{fl} = m_1 \cdot f_{BK}(\varepsilon, n) + const. \qquad \text{(Eq. 3)}$$

$$\nu_{abs} + \nu_{fl} = -m_2 \cdot \left[f_{BK}(\varepsilon, n) + 2 g_{BK}(n) \right] + const. \qquad \text{(Eq. 4)}$$

In the equations of Eq. 3 and Eq. 4, $f_{BK}(\varepsilon,n)$ and $g_{BK}(n)$ are solvent polarizability function, respectively. Using a slope of m_1 and m_2, and the calculated permanent dipole moment (μ_e and μ_g) can be obtained from Eq. 5 and 6. The a calculated from the absolute density of compound **1** was 5.98 Å.

$$m_1 = \frac{2(\mu_e - \mu_g)^2}{hca^3} \qquad \text{(Eq. 5)}$$

$$m_2 = \frac{2(\mu_e^2 - \mu_g^2)}{hca^3} \qquad \text{(Eq. 6)}$$

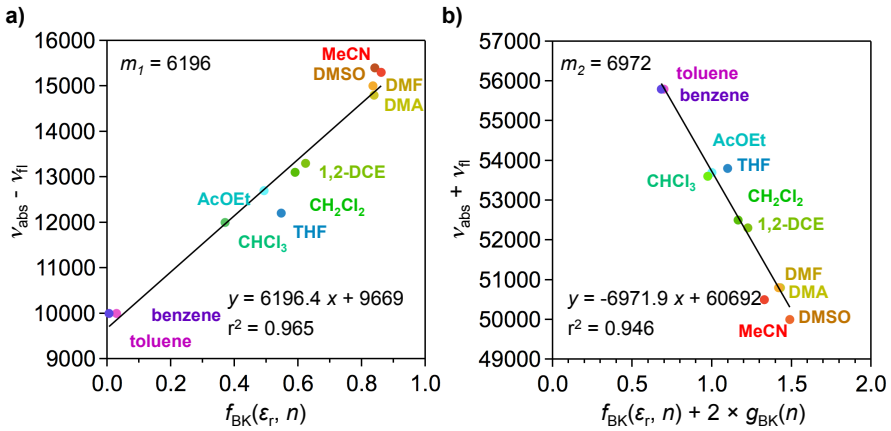

Fig. S10 Bilot-Kawski plots. Stokes shifts ($\nu_{abs} - \nu_{fl}$) *vs* orientation polarizability function $f_{BK}(\varepsilon,n)$ and $g_{BK}(n)$ for **1**. Only aprotic solvents were used.

Reichardt's E_T^N solvent polarity parameter

$$\nu_{abs} - \nu_{fl} = 11307.6\left[\left(\frac{\Delta\mu}{\Delta\mu_B}\right)^2\left(\frac{a_B}{a}\right)^3\right]E_T^N + const. \qquad \text{(Eq. 7)}$$

E_T^N is one of the most popular solvent polarity parameter obtained by molar electronic transition energies (E_T) of penta-*tert*-butyl-substituted betaine dye. In the equation of Eq. 7, $\Delta\mu_B$ is the dipole moment change of a pyridinium *N*-phenolate betaine dye ($\Delta\mu_B = 9$ D) ; a_B is the radius of the cavity in which the pyridinium *N*-phenolate betaine dye (a_B = 6.2 Å).

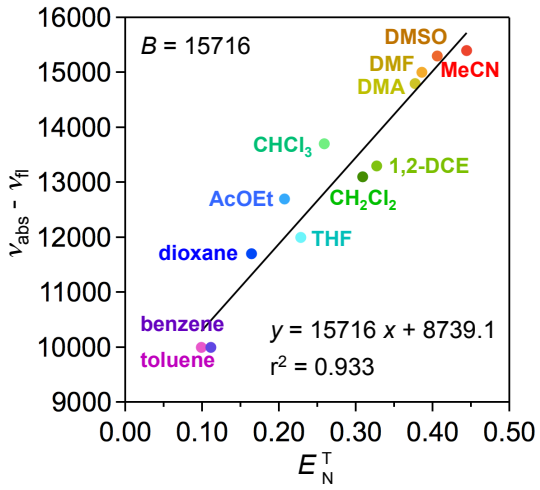

Fig. S11 Stokes shifts ($\nu_{abs} - \nu_{fl}$) *vs* E_T^N plot for **1**. Only aprotic solvents were used.

Table S1 Difference between the ground (μ_g) and excited (μ_e) permanent dipole moment of compound **1**.

1; $\mu_{g\,(calculated)}$ = 11.01 [D]*1, a = 5.98 [Å]		
Lippert-Mataga	μ_e = 28.31 [D] *2	$\Delta\mu$ = 17.30 [D]
Bilot-Kawski	μ_e = 16.37 [D] *2	$\Delta\mu$ = 5.36 [D]
E_T^N	μ_e = 20.82 [D] *2	$\Delta\mu$ = 9.81 [D]
DFT*1	μ_e = 20.54 [D] *2	$\Delta\mu$ = 9.53 [D]

*1 μ_g and μ_e were calculated by using the CAM-B3LYP/6-31G(d,p) level of theory.
*2 μ_e was estimated using $\mu_{g(calculated)}$.

5. Kinetics

In a typical experiment, 40 μM solutions of compound **1**, **8**, **9**, **11** and **14** were prepared in degassed $CHCl_3$ and the absorption spectra of the closed form were measured under nitrogen atmosphere. Photo-conversion of closed form of these compounds to zwitterionic form (**1Z**, **8Z**, **9Z**, **11Z** and **14Z**) was carried out by using xenon lamp (305 nm, 1500 W) coupled to HITACHI F-7100 fluorescence spectrophotometer equipped with a temperature controller unit. Thermal relaxation analysis of zwitterionic form was measured in water bath at 5℃ increments from 298 to 313 K over a period of 8 hours. The thermal relaxation typically followed first order kinetics.

First-order rate constants for thermal relaxation were determined by fitting absorbance to Eq. 1, where Abs is the absorbance at 480 nm (**1Z**, **9Z**, **11Z**, and **14Z**) or 510 nm (**8Z**), Abs_0 is the absorbance value at $t = 0$, k is the rate constant and t is time.

$$\ln [Abs] = [Abs_0]e^{-kt} \qquad \text{(Eq. 1)}$$

The Arrhenius equation, as shown in Eq. 2, was used to plot the linear temperature dependence of the rate constant for thermal relaxation and find the activation energy (E_a), the pre-exponential factor (A), and half-life time ($t_{1/2}$). In the equation, k is the rate constant; R is the gas constant; T is the temperature (K).

$$\ln k = E_a/RT + \ln A \qquad \text{(Eq. 2)}$$

The thermodynamic activation of properties were calculated using Eyring equation, as shown in Eq. 3 and 4. In the equation, k is the rate constant; $\Delta S^{\ddagger}$ is the entropy of activation; $\Delta H^{\ddagger}$ is the enthalpy of activation; R is the gas constant; T is the temperature (K); k_B is the Boltzmann constant; h is the Planck's constant; $K^{\ddagger}$ is the transition state equilibrium of activation.

$$\ln(k/T) = \ln(k/h) + \Delta S^{\ddagger}/R - \Delta H^{\ddagger}/RT \qquad \text{(Eq. 3)}$$

$$k = (k_B T/h)K^{\ddagger} \qquad \text{(Eq. 4)}$$

Eq. 5 was used to calculate the Gibbs free energy of activation ($\Delta G^{\ddagger}$).

$$\Delta G^{\ddagger} = \Delta H^{\ddagger} - T\Delta S^{\ddagger} \qquad \text{(Eq. 5)}$$

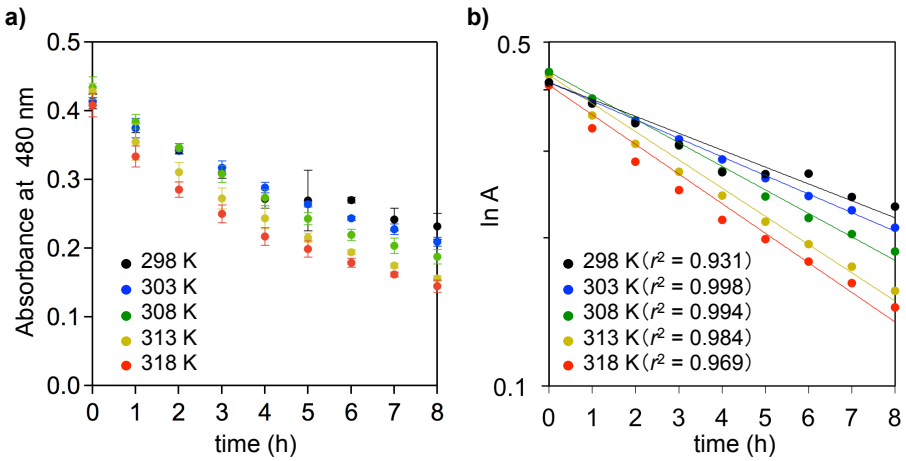

Fig. S12 (a) Thermal decay profiles of **1Z** monitored at 480 nm in degassed $CHCl_3$ under nitrogen atmosphere. The measurements were performed over the temperature range 298-318 K. (b) The ln A vs. time plots for the thermal bleaching process. The curves were fitted with first-order kinetics to calculate the thermal bleaching rate constant: $k_{298\ K}$ = 0.079 h^{-1}, $k_{303\ K}$ = 0.087 h^{-1}, $k_{308\ K}$ = 0.110 h^{-1}, $k_{313\ K}$ = 0.132 h^{-1}, $k_{318\ K}$ = 0.138 h^{-1}.

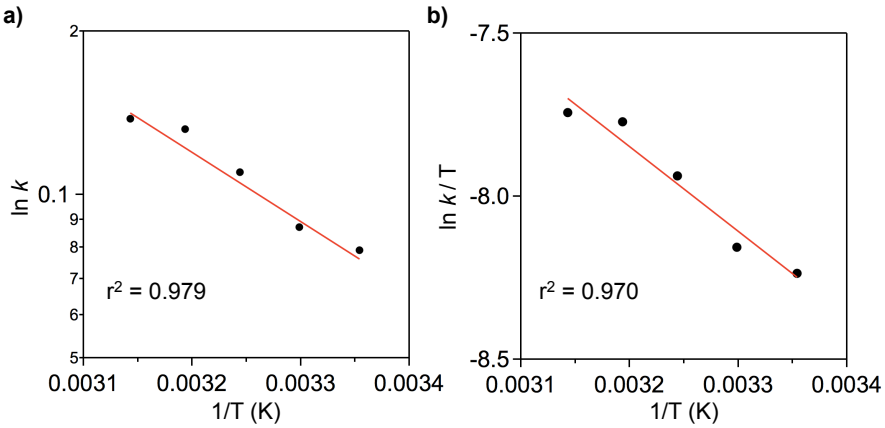

Fig. S13 (a) Arrhenius plots and (b) Eyring plots for the thermal bleaching process of **1Z**.

Table S2 Thermodynamic parameters associated with the thermal back reaction of **1Z** at 298 K.

$k_{298\ K}$	$t_{1/2}$	E_a	A	$\Delta H^{\ddagger}$	$\Delta S^{\ddagger}$	$\Delta G^{\ddagger}_{298\ K}$
H^{-1}	h	kcal mol^{-1}	H^{-1}	kcal mol^{-1}	cal mol^{-1} K^{-1}	kcal mol^{-1}
0.076	9.1	6.6	1.4×10^3	5.2	–46.2	18.8

$t_{1/2}$: half-life time, E_a: activation energy, A: pre-exponential factor, $\Delta H^{\ddagger}$: enthalpy of activation, $\Delta S^{\ddagger}$: entropy of activation, and $\Delta G^{\ddagger}_{298\ K}$: Gibbs energy of activation.

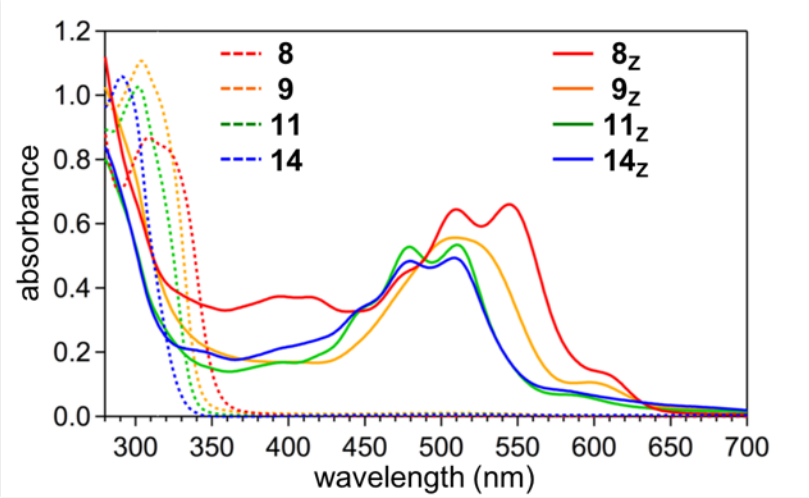

Fig. S14 Photoswitching of spiro-ring form to zwitterionic form of ABPXs with different electron donating amino substituents (**8**, **9**, **11** and **14**). Absorption spectra of 40 μM of **1** in $CHCl_3$ before (dotted line) and after (solid line) UV irradiation.

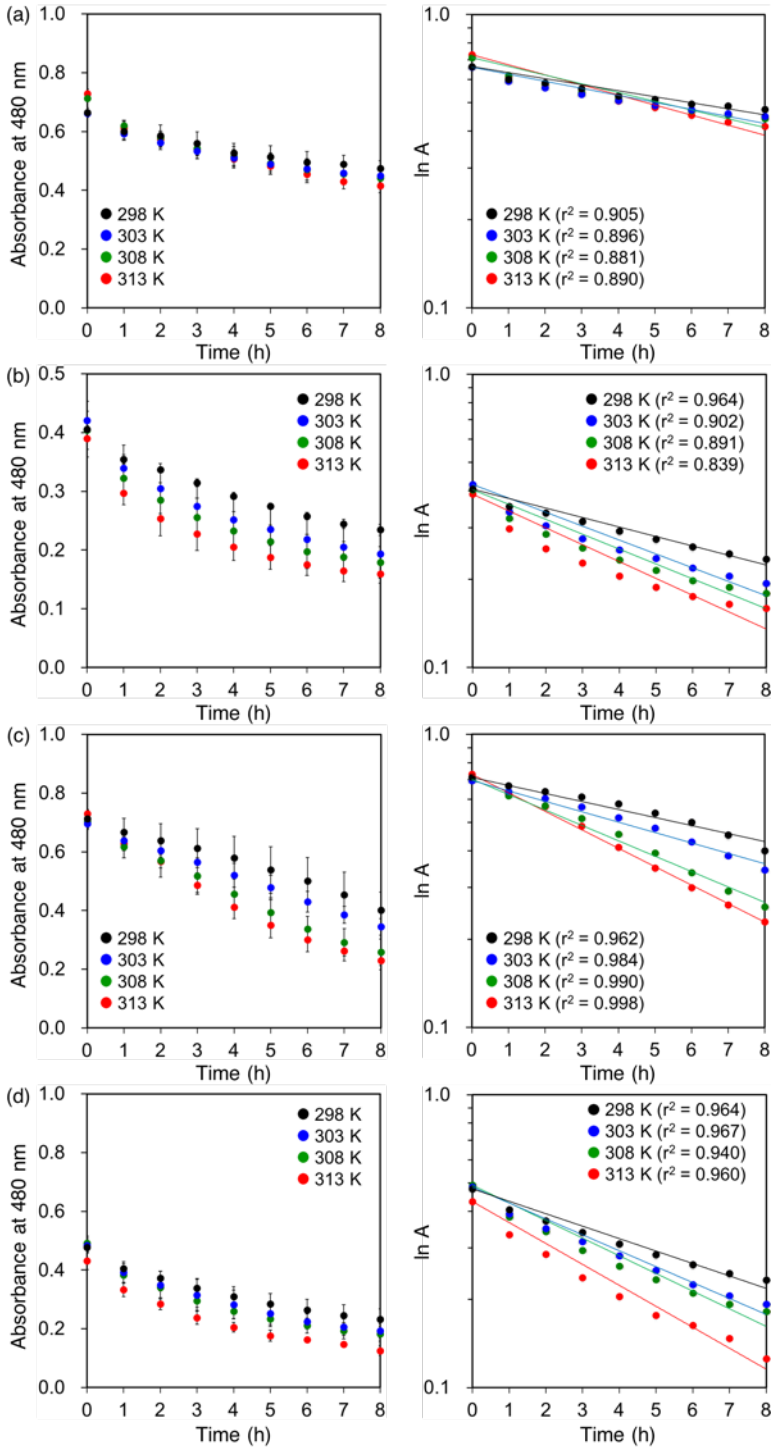

Fig. S15 (a) Thermal decay profiles of **8z**, **9z**, **11z**, and **14z** monitored at 480 nm in degassed $CHCl_3$ under nitrogen atmosphere. The measurements were performed over the temperature range 298-318 K. (b) The ln A vs. time plots for the thermal bleaching process. The curves were fitted with first-order kinetics to calculate the thermal bleaching rate constant.

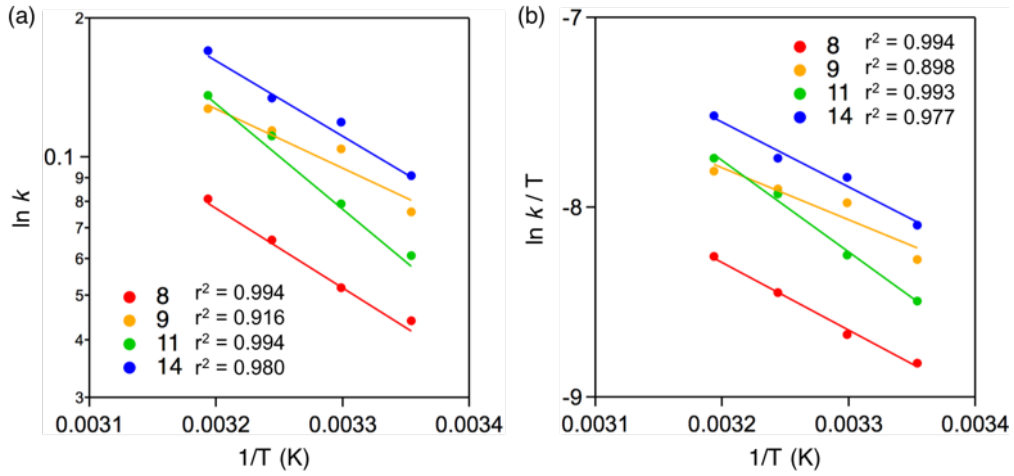

Fig. S16 (a) Arrhenius plots and (b) Eyring plots for the thermal bleaching process.

Table S3 Rate constants for thermal relaxation for **8**$_Z$, **9**$_Z$, **11**$_Z$, and **14**$_Z$ over 298-313 K averaged from 3 replicates.

	σ^+	$k_{298\ K}$ ($t_{1/2}$[h])	$k_{303\ K}$ ($t_{1/2}$[h])	$k_{308\ K}$ ($t_{1/2}$[h])	$k_{313\ K}$ ($t_{1/2}$[h])
8$_Z$	–2.03	0.044 (15.8)	0.052 (13.3)	0.066 (10.5)	0.081 (8.60)
9$_Z$	–1.80	0.076 (9.10)	0.104 (6.70)	0.114 (6.10)	0.127 (5.50)
11$_Z$	–1.70	0.061 (11.4)	0.079 (8.80)	0.111 (6.20)	0.136 (5.10)
14$_Z$	–1.51	0.091 (7.60)	0.119 (5.80)	0.134 (5.20)	0.170 (4.10)

Table S4 Thermodynamic parameters associated with the thermal back reaction of **8**$_Z$, **9**$_Z$, **11**$_Z$, and **14**$_Z$ at 313 K averaged from 3 replicates.

	σ^+	E_a kcal mol^{-1}	A H^{-1}	$\Delta H^{\ddagger}$ kcal mol^{-1}	$\Delta S^{\ddagger}$ cal mol^{-1} K^{-1}	$\Delta G^{\ddagger}_{313\ K}$ kcal mol^{-1}
8$_Z$	–2.03	7.7	1.8×10^4	7.1	–41.1	19.9
9$_Z$	–1.80	4.5	2.3×10^3	5.5	–45.2	19.6
11$_Z$	–1.70	10.2	2.0×10^6	9.6	–32.0	19.6
14$_Z$	–1.51	5.8	2.4×10^4	6.8	–40.6	19.5

6. Synthesis

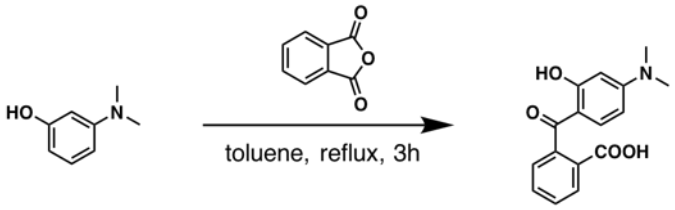

10

A suspension of *N,N*-diethyl-3-aminophenol (4.11 g, 30.0 mmol) and phthalic anhydride (4.69 g, 31.6 mmol) in toluene (30 mL) was refluxed under Ar for 3 h. Then 10 mL of 10 M aqueous NaOH was added in two steps and heated at 100℃ for 6 h. The resulting mixture was poured into H_2O (100 mL), acidified with HCl, and allowed to stand at room temperature for 2 h. The suspension was then dissolved in $CHCl_3$. Then extraction was carried out H_2O three times. The organic phase was dried over $MgSO_4$ and evaporated to the crude product. This was purified by silica gel column chromatography to obtain the pure product of **4c** as brown powder. Yield: 7.9 g (87%).

Compound 10: ^{1}H-NMR ($CDCl_3$, 400 MHz): δ 12.49 (s, 1 H), 8.08 (dd, 1 H, *J* = 7.9, 1.3 Hz), 7.62 (ddd, 1 H, *J* = 7.5, 7.5, 1.2 Hz), 7.52 (ddd, 1 H, *J* = 7.7, 7.7, 1.5 Hz), 7.35 (dd, 1 H, *J* = 7.5, 1.3 Hz), 6.88 (d, 1 H, *J* = 9.2 Hz), 6.15 (d, 1 H, *J* = 2.2 Hz), 6.06 (dd, 1 H, *J* = 9.2, 2.6 Hz), 3.02 (s, 6 H). These values of ^{1}H NMR of this compound were consistent with literature's one[2].

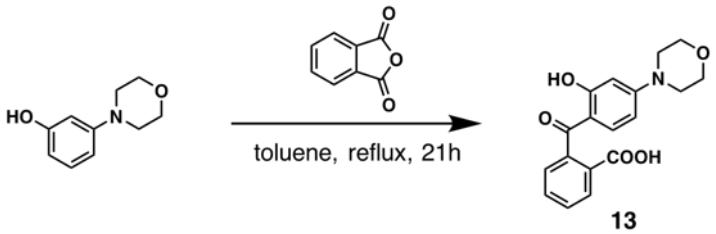

13

A suspension of **3c** (5.00 g, 27.9 mmol) and phthalic anhydride (6.22 g, 42.0 mmol) in toluene (10 mL) was refluxed under Ar for 21 h. Then 10 mL of 10 M aqueous NaOH was added in two steps and heated at 100℃ for 5 h. The resulting mixture was poured into H_2O (100 mL), acidified with HCl, and allowed to stand at room temperature for 2 h. The suspension was then dissolved in $CHCl_3$. Then extraction was carried out H_2O three times. The organic phase was dried over $MgSO_4$ and evaporated to the crude product. This was purified by silica gel column chromatography to obtain the pure product of **4c** as yellow viscous oil. Yield: 4.7 g (52%).

Compound 13: ^{1}H-NMR ($CDCl_3$, 400 MHz): δ 12.4 (s, 1 H), 8.11 (dd, 1 H, *J* = 7.8, 1.4

Hz), 7.66 (ddd, 1 H, J = 7.8, 7.6, 1.4 Hz), 7.56 (ddd, 1 H, J = 7.6, 7.6, 1.4 Hz), 7.36 (dd, 1 H, J = 7.6, 1.4 Hz), 6.93 (d, 1 H, J = 9.0 Hz), 6.36 (d, 1 H, J = 2.5 Hz), 6.23 (dd, 1 H, J = 9.0, 2.5 Hz), 3.81 (m, 4 H), 3.32 (m, 4 H). ^{13}C-NMR ($CDCl_3$, 400 MHz): δ 199.37, 170.09, 165.08, 156.45, 140.92, 134.22, 132.95, 131.06, 129.41, 127.81, 127.59, 112.07, 105.34, 100.18, 66.40, 46.79. HRMS (ESI, positive mode): m/z calcd for $C_{18}H_{17}NO_5$ $[M+H]^+$ 328.1179; Found 328.1179.

General procedure for the synthesis of ABPXs

A solution of benzophenone derivatives **10** or **13** (2.0 eq.) and resorcinol (1.0 eq) in CH_3SO_3H were heated at 110ºC for 6 h in a sealed tube. On cooling, the mixture was poured into ice and its pH was adjusted to 9~11 with aqueous NaOH followed by extraction with $CHCl_3$. The organic layers were dried over $MgSO_4$ and evaporated to give the crude product. This was purified by thin-layer silica gel chromatography to obtain the pure product *trans*-isomer was firstly eluted, followed by *cis*-isomer.

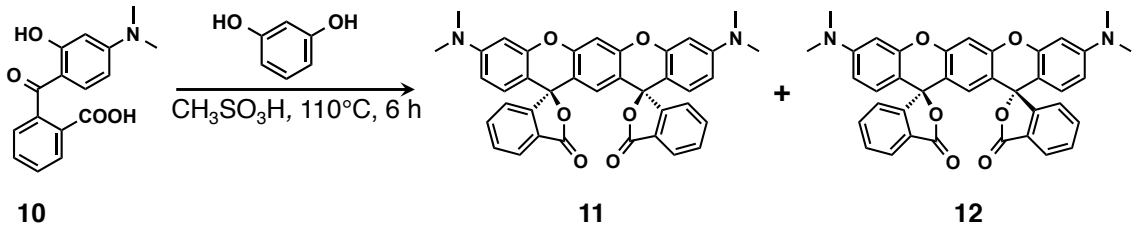

10 **11** **12**

Compound 11: Yield 49 %. ^{1}H NMR ($CDCl_3$, 400 MHz): δ 7.84-7.82 (m, 2 H), 7.45-7.42 (m, 4 H), 7.15 (s, 1 H), 6.92-6.90 (m, 2 H), 6.53-6.51 (m, 4 H), 6.38 (dd, 2 H, J = 9.0, 2.5 Hz), 6.00 (s, 1 H), 2.99 (s, 12 H) ^{13}C NMR ($CDCl_3$, 100 MHz): δ 168.95, 168.12, 164.23, 153.30, 152.84, 152.30, 144.72, 134.27, 129.42, 128.63, 128.58, 127.23, 125.07, 123.76, 123.47, 122.61, 116.41, 113.89, 109.13, 106.61, 92.24, 40.38 HRMS (ESI, positive mode): m/z calcd. for $C_{42}H_{33}O_8^+$ $[M]^+$

Compound 12: Yield 38 %. ^{1}H NMR ($CDCl_3$, 400 MHz): δ 7.80 (dd, 2 H, J = 7.6, 0.9 Hz), 7.61 (ddd, 2 H, J = 7.6, 7.4, 1.2 Hz), 7.52 (ddd, 2 H, J = 7.5, 7.5, 0.9 Hz), 7.14 (s, 1 H), 7.11 (dd, 2 H, J = 7.7, 0.8 Hz), 6.54-6.52 (m, 4 H), 6.39 (dd, 2 H, J = 8.9, 2.6 Hz), 6.07 (s, 1 H), 2.99 (s, 12 H) ^{13}C NMR ($CDCl_3$, 100 MHz): δ 169.33, 153.24, 153.58, 152.30, 152.28, 135.25, 129.87, 128.61, 127.89, 126.60, 124.73, 124.03, 116.40, 109.17, 106.09, 104.37, 102.73, 98.67, 83.38, 40.36, 28.25 HRMS (ESI, positive mode): m/z calcd. for $C_{42}H_{33}O_8^+$ $[M]^+$

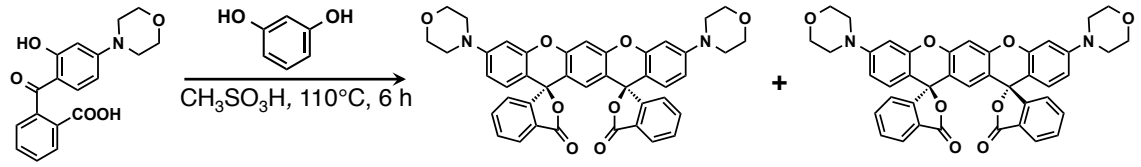

13 14 15

Compound 14: Yield 32%. ^{1}H NMR ($CDCl_3$, 600 MHz): δ 7.86-7.85 (m, 2 H), 7.57-7.54 (m, 4 H), 7.18 (s, 1 H), 6.92-6.91 (m, 2 H), 6.75 (d, 2 H, *J* = 1.2 Hz), 6.59 (d, 4 H, *J* = 1.2 Hz), 6.05 (s, 1 H), 3.87 (dd, 8 H, *J* = 5.0, 5.0 Hz), 3.22 (dd, 8 H, *J* = 5.0, 5.0 Hz). ^{13}C NMR ($CDCl_3$, 150 MHz): δ 168.76, 153.11, 152.54, 152.10, 134.29, 129.49, 128.54, 128.50, 126.86, 125.09, 123.28, 116.35, 111.68, 109.46, 104.47, 101.85, 82.28, 66.63, 48.25, 29.78. HRMS (ESI, positive mode): m/z calcd. for $C_{42}H_{33}O_8^+$ $[M]^+$ 693.2231; Found 693.2210.

Compound 15: Yield 33%. ^{1}H NMR ($CDCl_3$, 600 Hz): δ 7.83 (dd, 2 H, *J* = 7.8, 0.9 Hz), 7.64 (ddd, 2 H, *J* = 7.8, 7.6, 1.2 Hz), 7.55 (ddd, 2 H, *J* = 7.6, 7.6, 0.9 Hz), 7.17 (s, 1 H), 7.12 (dd, 2 H, *J* = 7.6, 1.2 Hz), 6.75 (d, 2 H, *J* = 0.9 Hz), 6.60 (m, 4 H), 6.12 (s, 1 H), 3.87 (dd, 8 H, *J* = 5.0, 5.0 Hz), 3.23 (dd, 8 H, *J* = 5.0, 5.0 Hz). ^{13}C-NMR ($CDCl_3$, 600 MHz): δ 169.03, 153.07, 152.96, 152.30, 152.12, 135.26, 129.93, 128.55, 127.78, 126.19, 124.79, 123.82, 116.36, 111.73, 109.36, 104.42, 101.81, 82.49, 66.63, 48.23. HRMS (ESI, positive mode): m/z calcd. for $C_{42}H_{33}O_8^+$ $[M]^+$ 693.2231; Found 693.2216.

7. Crystallographic data collection and structure refinement

Single crystals of compounds **2** and **3** were obtained by slow diffusion of less solubilizing solvent vapor (Et_2O) into more solubilizing solvent (THF). Crystal data and structure refinement for these crystals are summarized in Table S5. X-ray diffraction data were collected on a Rigaku Varimax with Saturn using Mo Kα radiation (λ = 0.710747 Å) at 110 K. Frame data were integrated and the data set was corrected for absorption using a Rigaku/MSC CrystalClear program package. All calculations were performed with a Rigaku/MSC CrystalStructure program package, and structures were solved by Direct Methods (SIR2011)[3] and refined on F^2 by full-matrix least squares techniques (SHELXL 2013)[4]. Anisotropic refinement was applied to all non-hydrogen atoms, and all hydrogen atoms were put at the calculated positions. Structural drawings and geometrical calculations were performed with ORTEP[5] and PLATON[6], respectively. Crystallographic data for these crystals were deposited with the Cambridge Crystallographic Data Centre (CCDC). The data can be obtained free of charge from the CCDC *via* www.ccdc.cam.ac.uk/data_request/cif.

Table S5 Crystal data and structure refinement for compounds **2** and **3**.

	2	**3**
Chemical formula	$C_{43}H_{37}N_3O_6$	$C_{50}H_{51}N_3O_7$
Formula Weight	691.78	805.97
Crystal Color, Habit	red, prism	colorless, prism
Crystal Dimensions	0.230×0.220×0.200 mm	0.170×0.150×0.140 mm
crystal system	monoclinic	monoclinic
space group [No.]	P21/c	P21/n
a, Å	14.527(3)	9.9387(13)
b, Å	16.277(3)	13.4852(11)
c, Å	16.006(3)	31.896(3)
α, °	90	90
β, °	106.414(7)	92.127(5)
γ, °	90	90
volume, Å^3	3630.5(12)	4271.9(8)
Z	4	4
D_{calcd}, g/cm^3	1.266	1.253
T, K	110	110
radiation[a]	MoKα	MoKα
$2\theta_{max}$, °	54.9	55.0
F(000)	1456.00	1712.00
reflns collected	54103	56836
unique reflns	8218	9394
R1 factor (I > 2.00σ(I))	0.0808	0.0909
R factor (all reflection)	0.1341	0.1252
wR factor	0.2973	0.3025
GOF	0.946	1.179
CCDC No.	1879131	1879130

8. Computational details

Density functional calculations were performed with the Gaussian 09 program package.[7] Geometry optimisation for the S_0 and S_1 state was performed at the CAM-B3LYP density functional[8] and the 6-31G** basis sets. Electrostatic potential (ESP) maps were drawn by GaussView 5. ESP surfaces were generated at an isodensity value of 4.0×10^{-4} electron/bohr^3 and surface potential range was set to –44 (red) and 28 kcal/mol (blue).

9. NMR spectra

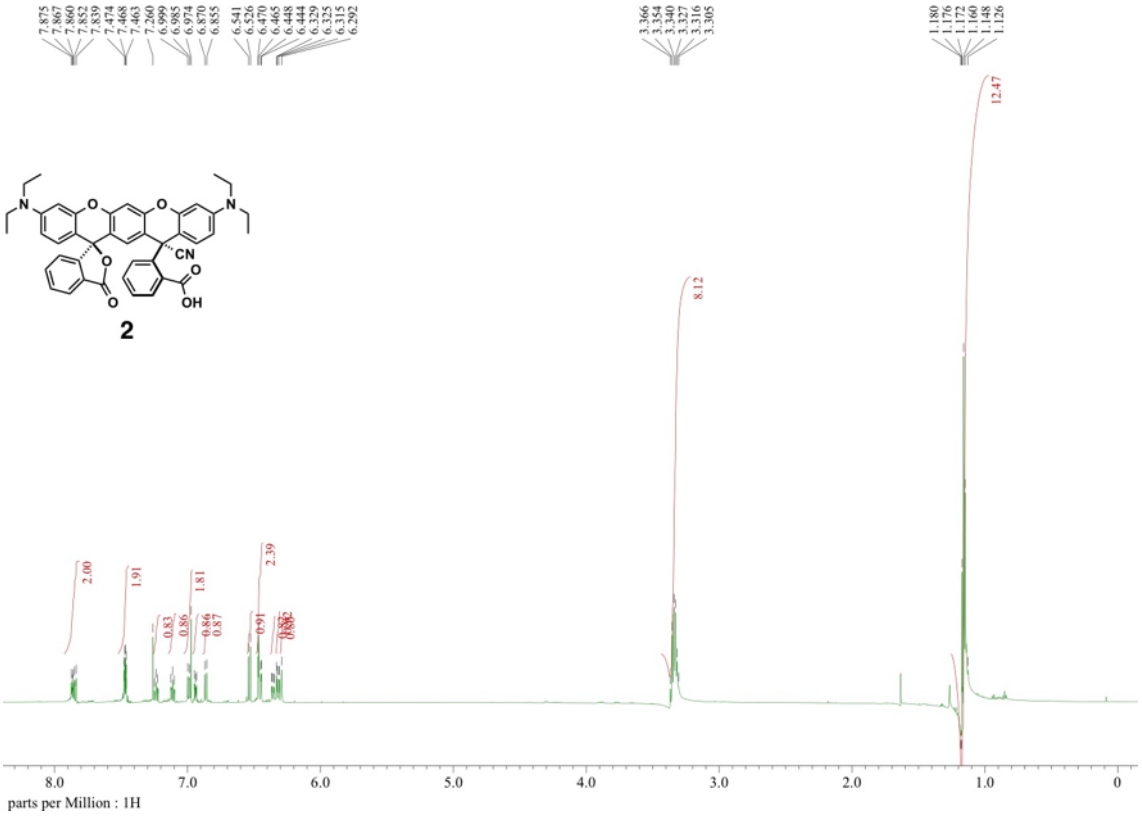

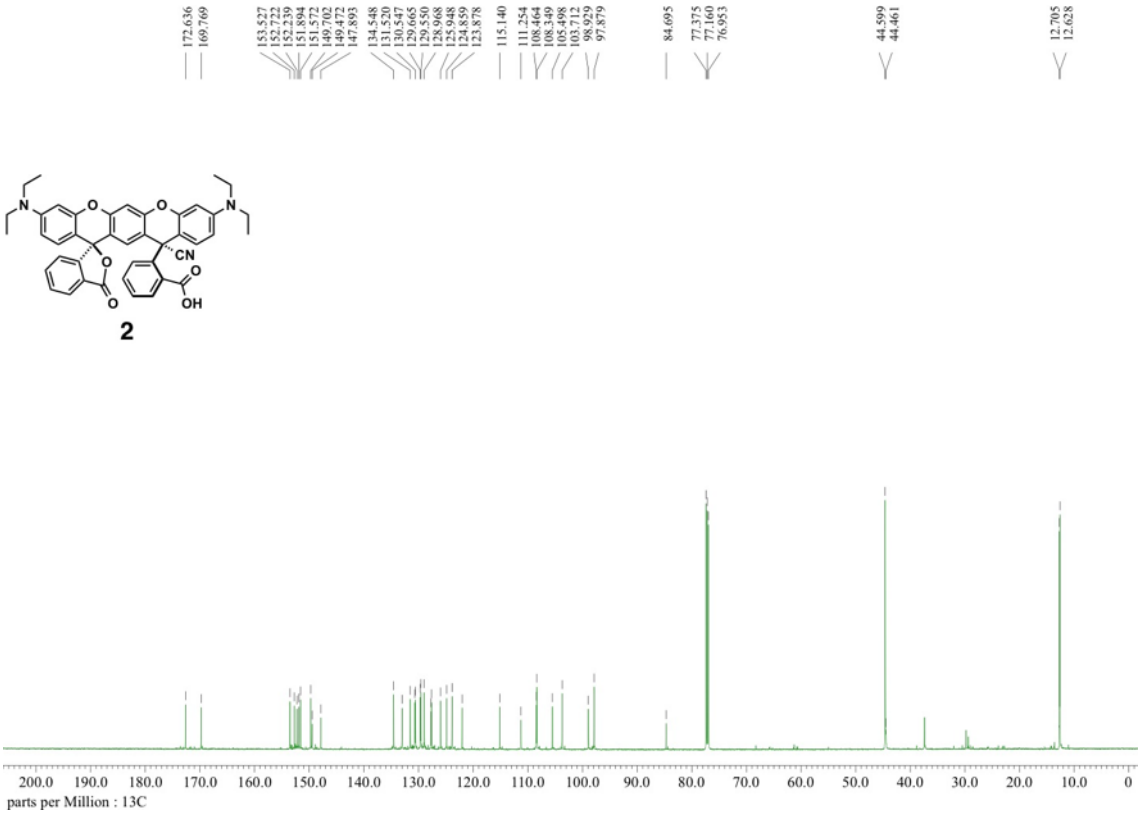

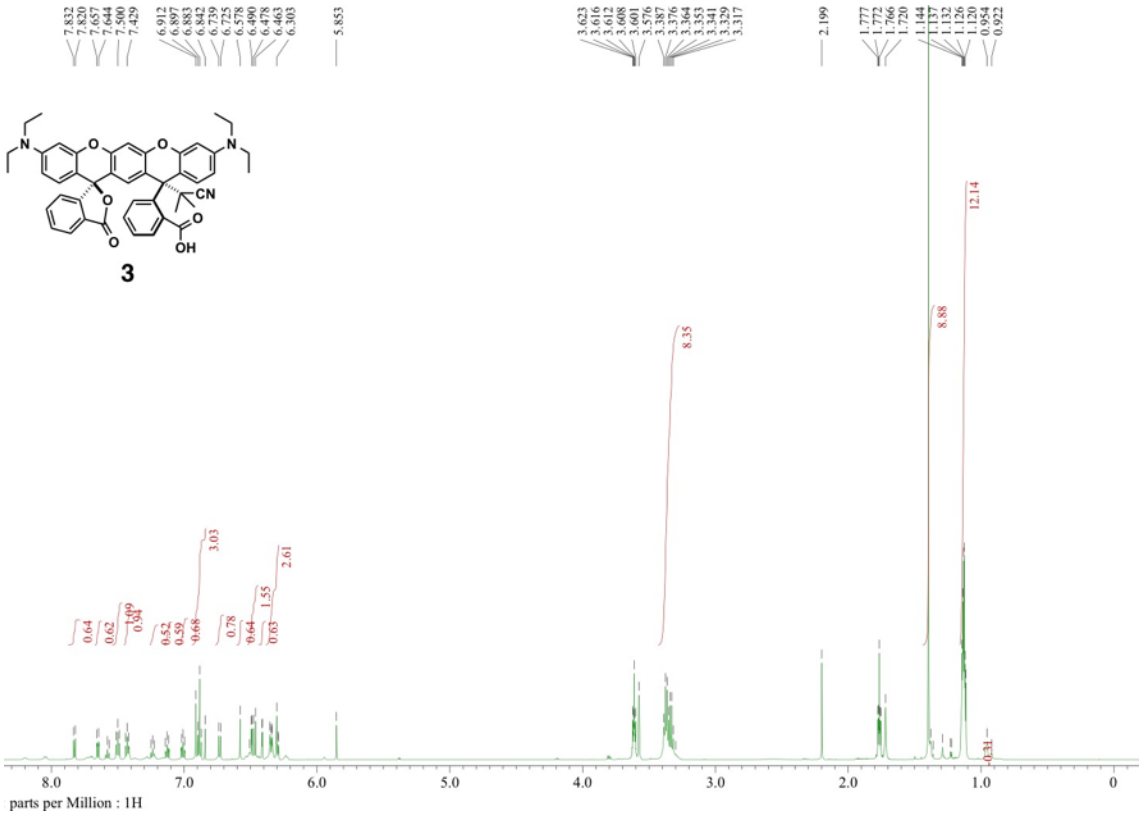
7.832
7.830
7.657
7.644
7.500
7.429
6.912
6.897
6.883
6.842
6.739
6.725
6.578
6.490
6.478
6.463
6.303
5.853
3.623
3.616
3.612
3.608
3.601
3.576
3.387
3.376
3.364
3.353
3.341
3.329
3.317
2.199
1.777
1.772
1.766
1.720
1.144
1.137
1.132
1.126
1.120
0.954
0.922
CN
O
OH
3
8.35
8.88
12.14
3.03
2.61
1.55
0.64
0.62
1.09
0.94
0.52
0.50
0.68
0.78
0.64
0.63
0.31
8.0
7.0
6.0
5.0
4.0
3.0
2.0
1.0
0
parts per Million : 1H

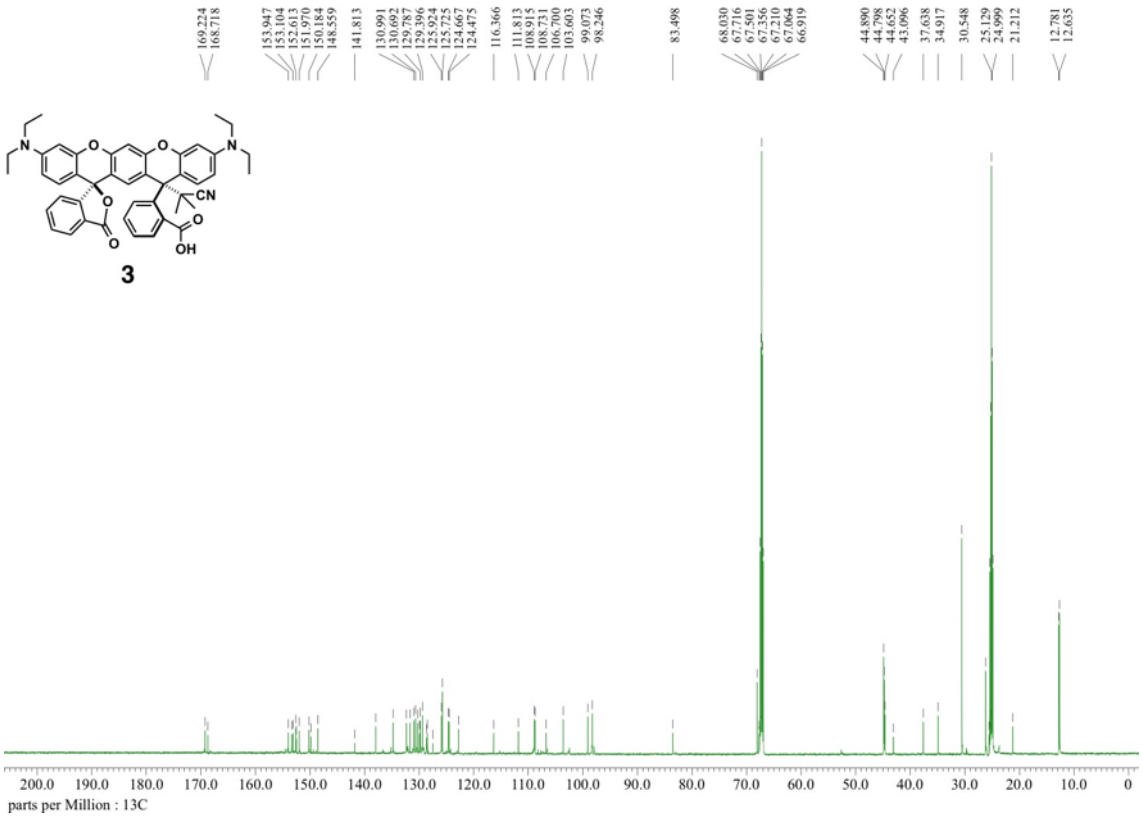
169.224
168.718
153.947
153.104
152.613
151.970
150.384
148.559
141.813
130.991
130.692
129.787
129.396
125.924
125.725
124.667
124.475
116.366
111.813
108.915
108.731
106.700
103.603
99.073
98.246
83.498
68.030
67.716
67.501
67.356
67.210
67.064
66.919
44.890
44.798
44.652
43.096
37.638
34.917
30.548
25.129
24.999
21.212
12.781
12.635
CN
O
OH
3
200.0
190.0
180.0
170.0
160.0
150.0
140.0
130.0
120.0
110.0
100.0
90.0
80.0
70.0
60.0
50.0
40.0
30.0
20.0
10.0
0
parts per Million : 13C

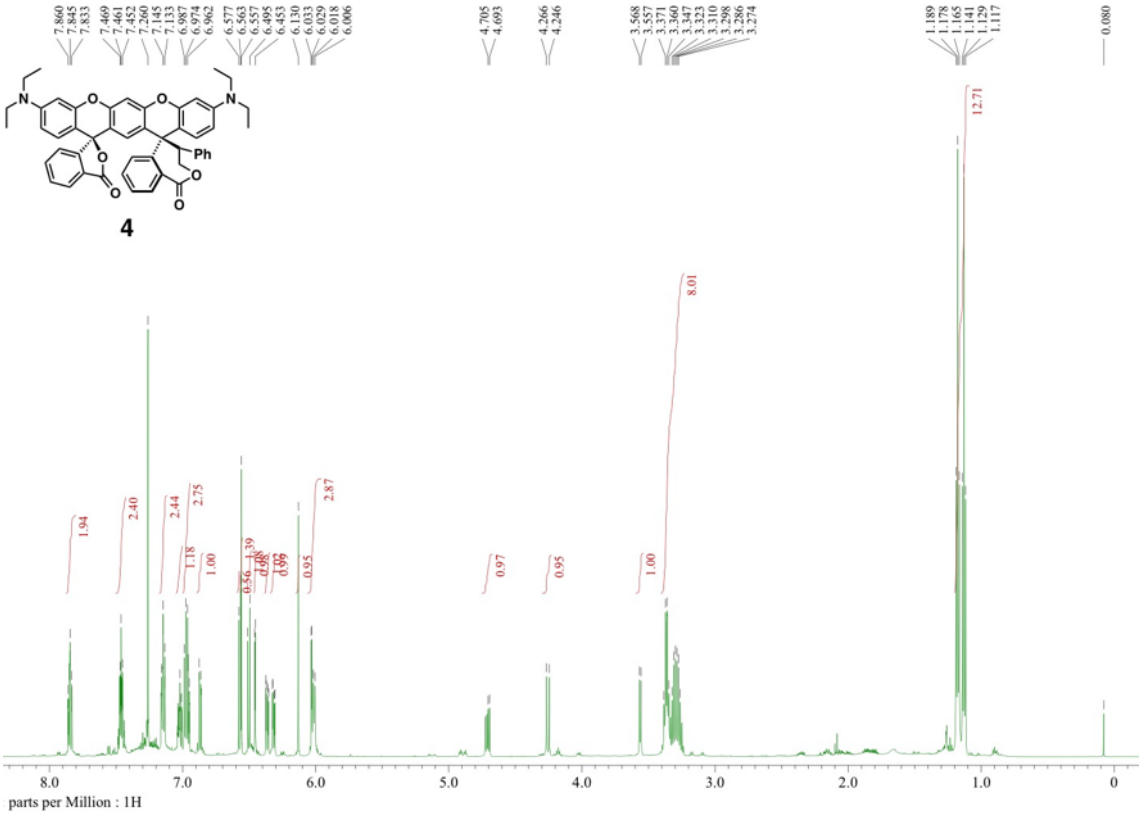
7.860
7.845
7.833
7.469
7.461
7.452
7.260
7.145
7.133
6.987
6.974
6.962
6.577
6.563
6.557
6.495
6.453
6.130
6.033
6.029
6.018
6.006
4.705
4.693
4.266
4.246
3.568
3.557
3.371
3.360
3.347
3.323
3.310
3.298
3.286
3.274
1.189
1.178
1.165
1.141
1.129
1.117
0.080
Ph
O
N
4
12.71
8.01
2.87
2.75
2.44
2.40
1.94
1.39
1.18
1.00
0.97
0.95
0.95
1.00
8.0
7.0
6.0
5.0
4.0
3.0
2.0
1.0
0
parts per Million : 1H

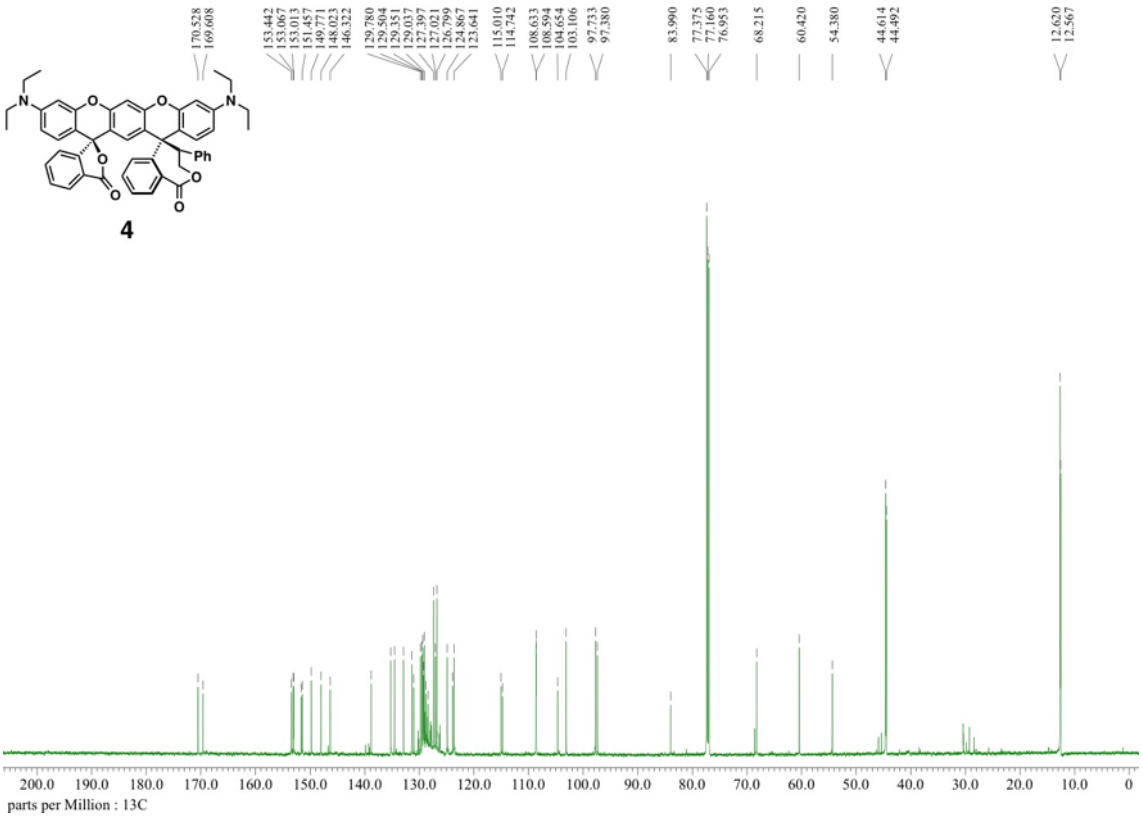
170.528
169.608
153.442
153.067
153.013
151.457
149.771
148.023
146.322
129.780
129.504
129.351
129.037
127.397
127.021
126.799
124.867
123.641
115.010
114.742
108.633
108.594
104.654
103.106
97.733
97.380
83.990
77.375
77.160
76.953
68.215
60.420
54.380
44.614
44.492
12.620
12.567
Ph
O
N
4
200.0
190.0
180.0
170.0
160.0
150.0
140.0
130.0
120.0
110.0
100.0
90.0
80.0
70.0
60.0
50.0
40.0
30.0
20.0
10.0
0
parts per Million : 13C

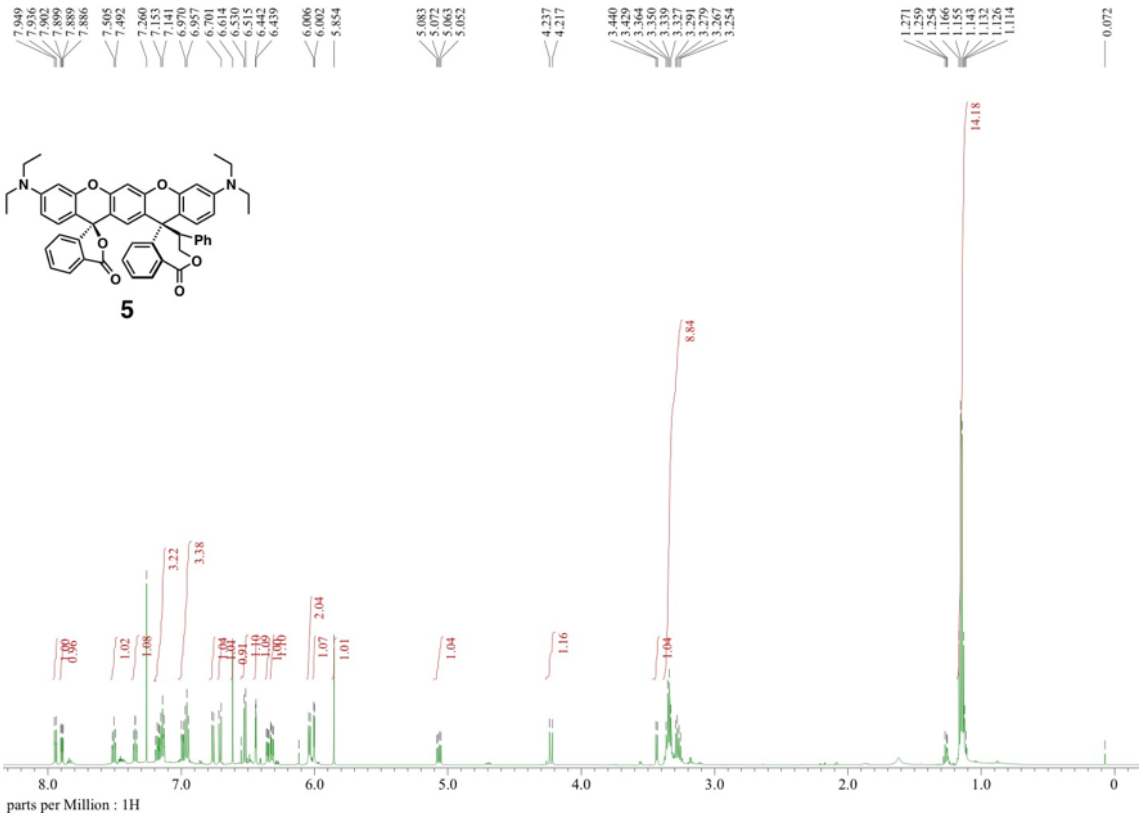
7.949
7.936
7.902
7.899
7.889
7.886
7.505
7.492
7.260
7.153
7.141
6.970
6.957
6.701
6.614
6.530
6.515
6.442
6.439
6.006
6.002
5.854
5.083
5.072
5.063
5.052
4.237
4.217
3.440
3.429
3.369
3.364
3.350
3.339
3.327
3.291
3.279
3.267
3.254
1.271
1.259
1.254
1.166
1.155
1.143
1.132
1.126
1.114
0.072
14.18
8.84
3.22
3.38
2.04
1.07
1.01
1.04
1.16
1.04
1.02
1.08
1.04
1.03
0.91
1.10
1.09
1.06
1.00
0.96
Ph
O
O
O
O
N
N
8.0
7.0
6.0
5.0
4.0
3.0
2.0
1.0
0
parts per Million : 1H

5

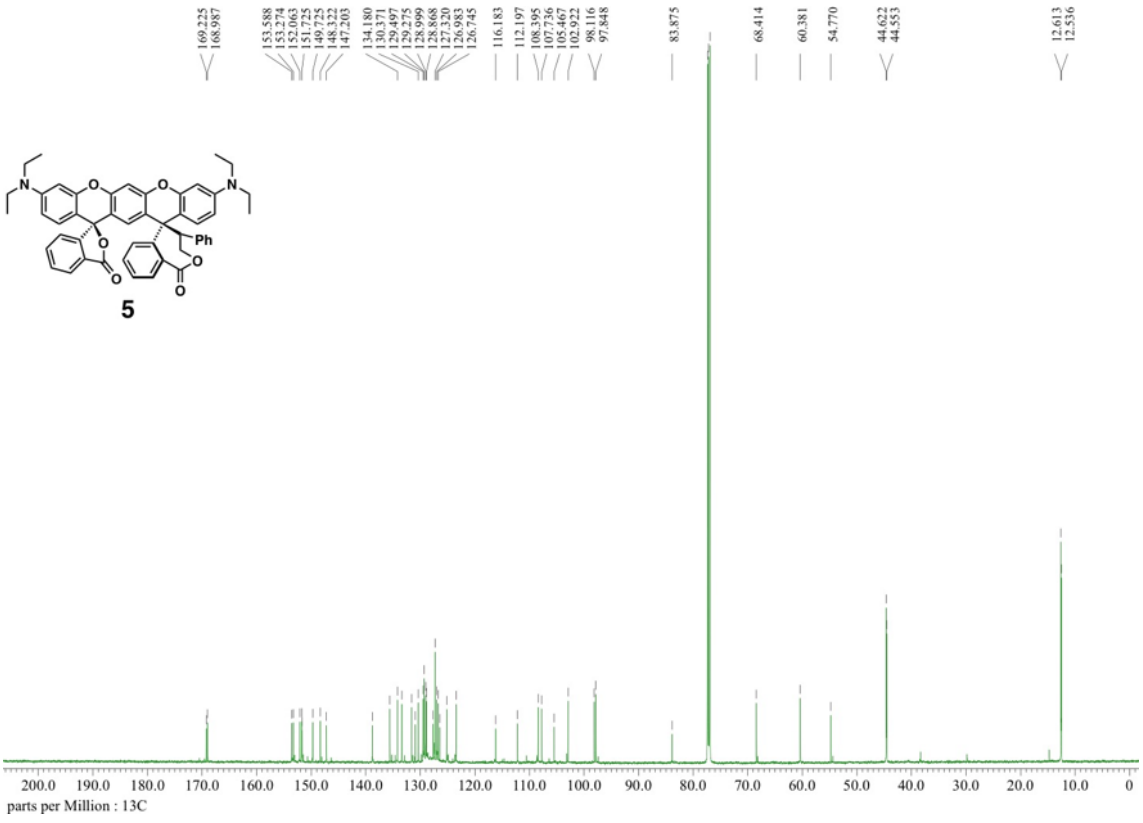
169.225
168.987
153.588
153.274
152.063
151.725
149.725
148.322
147.203
134.180
130.371
129.497
129.275
128.999
128.868
127.320
126.983
126.745
116.183
112.197
108.395
107.736
105.467
102.922
98.116
97.848
83.875
68.414
60.381
54.770
44.622
44.553
12.613
12.536
Ph
O
O
O
O
N
N
200.0
190.0
180.0
170.0
160.0
150.0
140.0
130.0
120.0
110.0
100.0
90.0
80.0
70.0
60.0
50.0
40.0
30.0
20.0
10.0
0
parts per Million : 13C

5

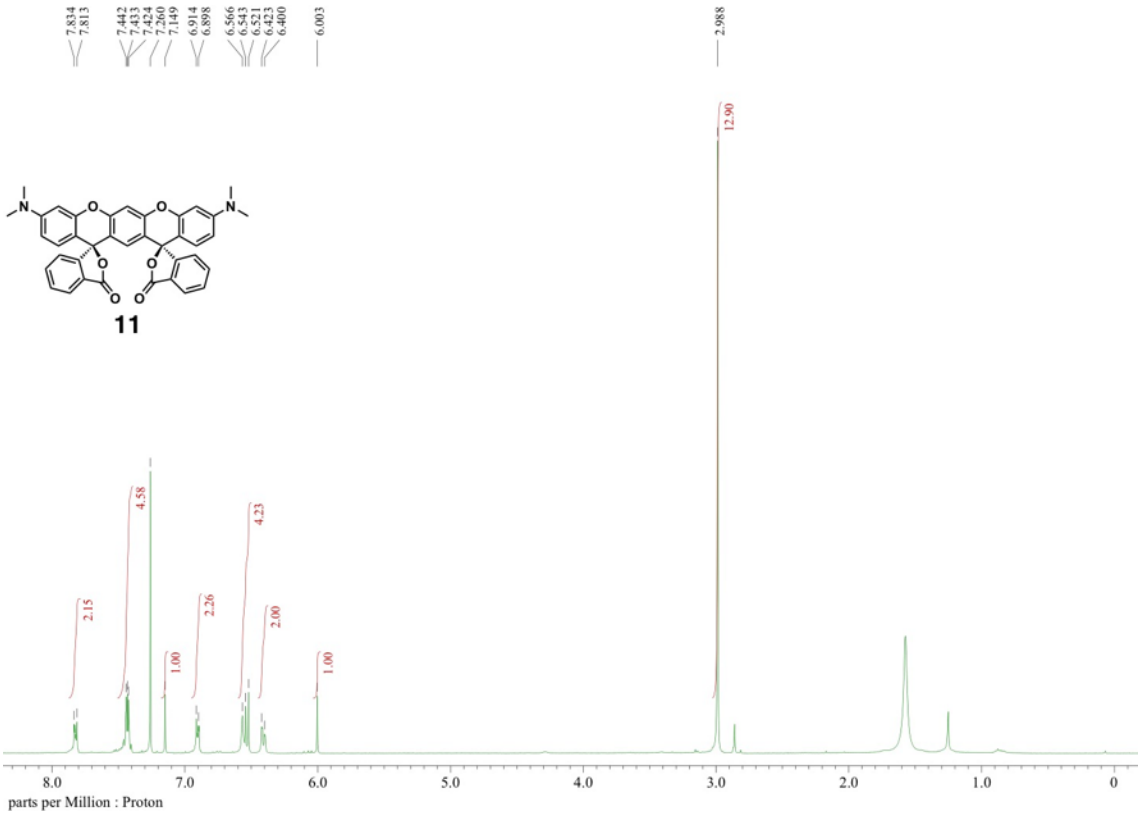
7.834
7.813
7.442
7.433
7.424
7.260
7.149
6.914
6.898
6.566
6.543
6.521
6.423
6.400
6.003
2.988
12.90
4.58
4.23
2.15
2.26
2.00
1.00
1.00
8.0
7.0
6.0
5.0
4.0
3.0
2.0
1.0
0
parts per Million : Proton

11

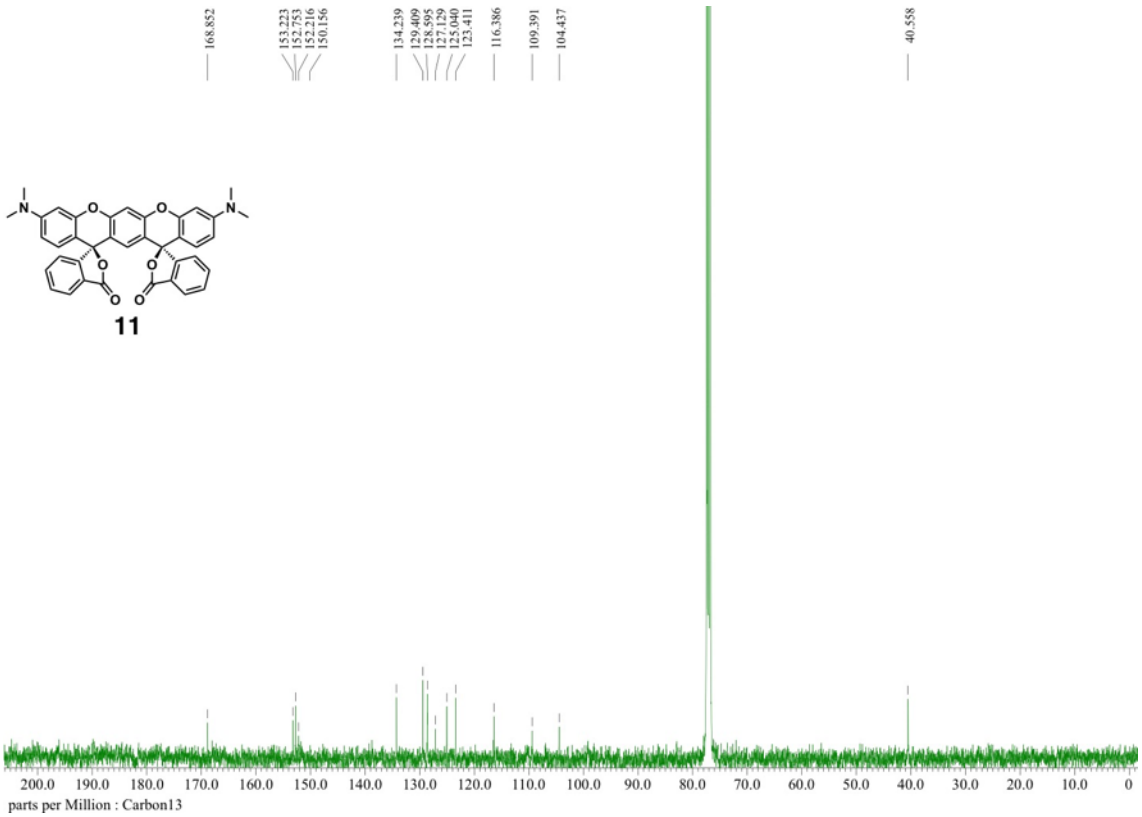
168.852
153.223
152.753
152.216
150.156
134.239
129.409
128.595
127.129
125.040
123.411
116.386
109.391
104.437
40.558
200.0
190.0
180.0
170.0
160.0
150.0
140.0
130.0
120.0
110.0
100.0
90.0
80.0
70.0
60.0
50.0
40.0
30.0
20.0
10.0
0
parts per Million : Carbon13

11

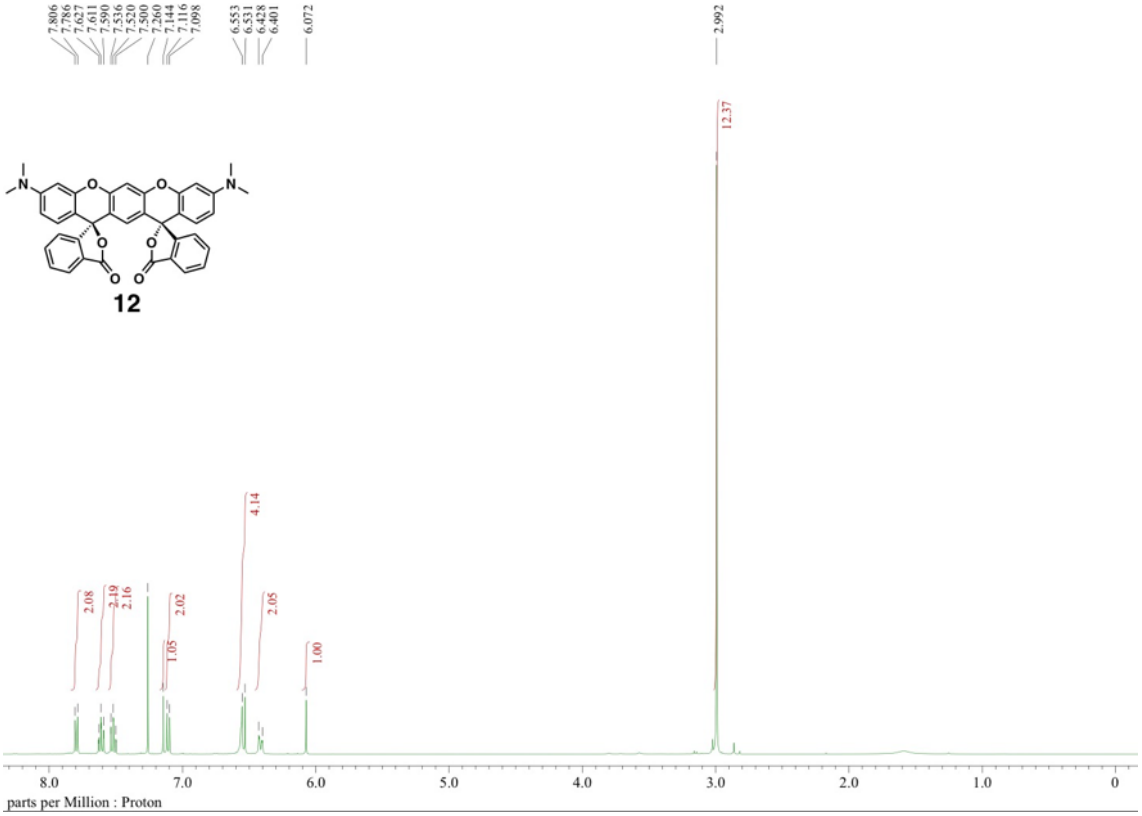
7.806
7.786
7.627
7.611
7.590
7.536
7.520
7.500
7.260
7.144
7.116
7.098
6.553
6.531
6.428
6.401
6.072
2.992
12.37
4.14
2.08
2.19
2.16
2.02
1.05
2.05
1.00
8.0
7.0
6.0
5.0
4.0
3.0
2.0
1.0
0
parts per Million : Proton

12

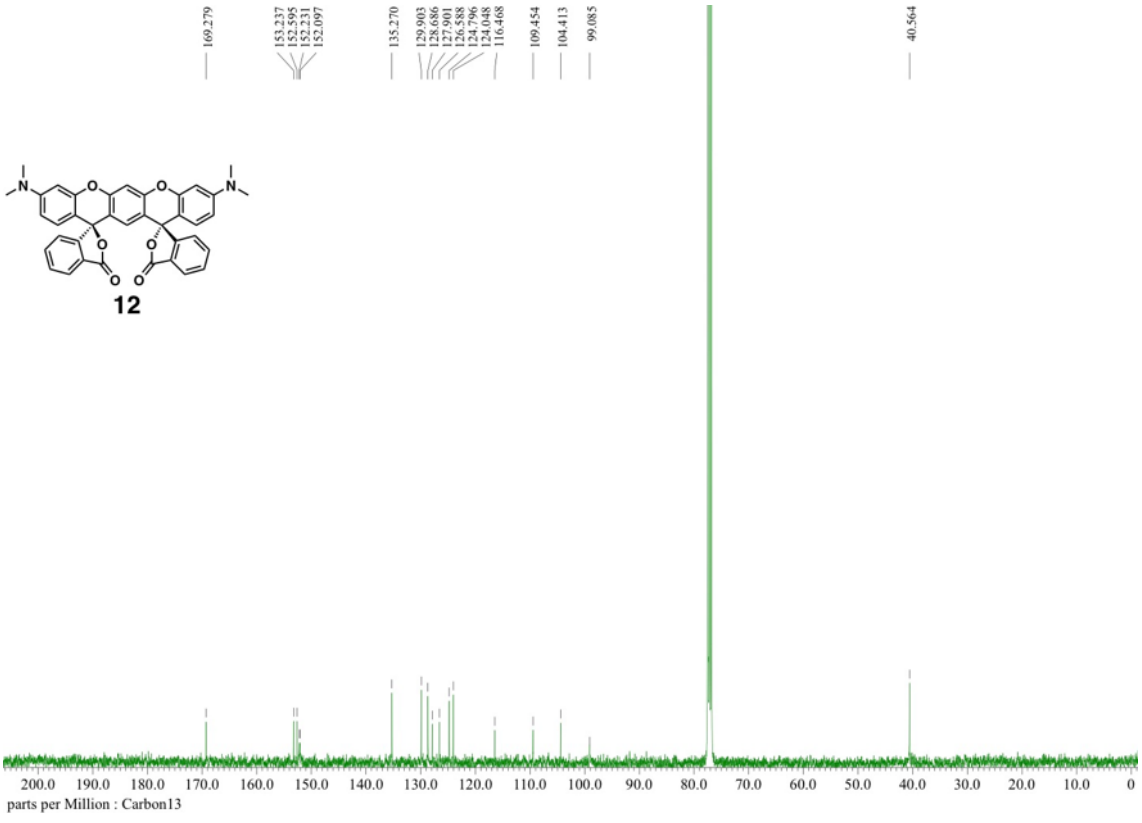
169.279
153.237
152.595
152.231
152.097
135.270
129.903
128.686
127.901
126.588
124.796
124.048
116.468
109.454
104.413
99.085
40.564
200.0
190.0
180.0
170.0
160.0
150.0
140.0
130.0
120.0
110.0
100.0
90.0
80.0
70.0
60.0
50.0
40.0
30.0
20.0
10.0
0
parts per Million : Carbon13

12

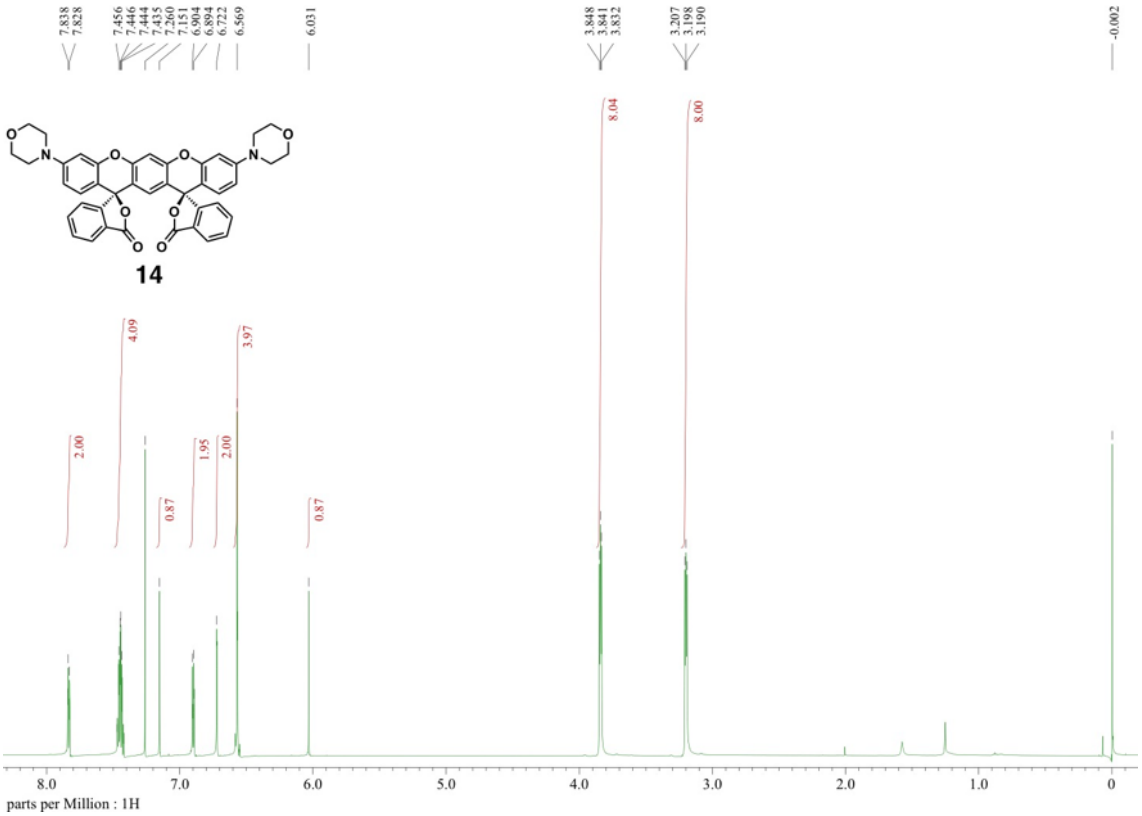
7.838
7.828
7.456
7.446
7.444
7.435
7.260
7.151
6.904
6.894
6.722
6.569
6.031
3.848
3.841
3.832
3.207
3.198
3.190
-0.002
8.04
8.00
4.09
3.97
2.00
1.95
2.00
0.87
0.87
8.0
7.0
6.0
5.0
4.0
3.0
2.0
1.0
0
parts per Million : 1H

14

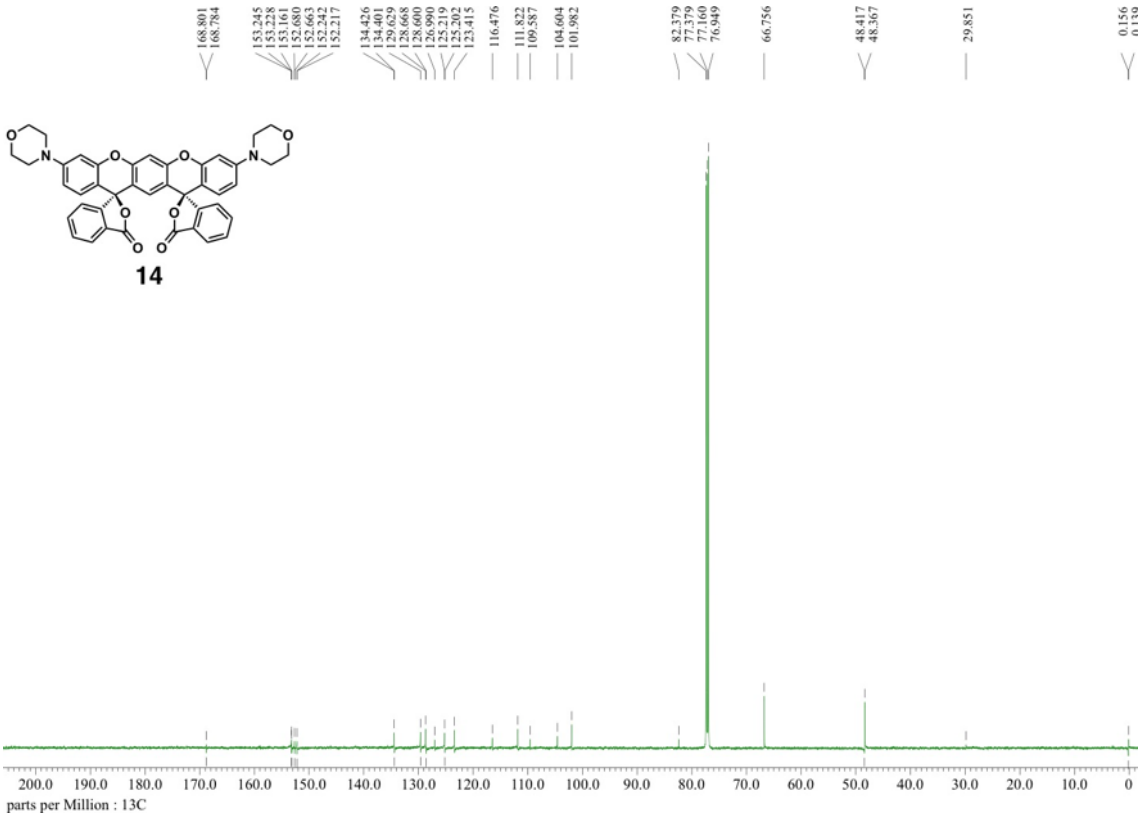
168.801
168.784
153.245
153.228
153.161
152.680
152.663
152.242
152.217
134.426
134.401
129.629
128.668
128.600
125.219
125.202
123.415
116.476
111.822
109.587
104.604
101.982
82.379
77.379
77.160
76.949
66.756
48.417
48.367
29.851
0.156
200.0
190.0
180.0
170.0
160.0
150.0
140.0
130.0
120.0
110.0
100.0
90.0
80.0
70.0
60.0
50.0
40.0
30.0
20.0
10.0
0
parts per Million : 13C

14

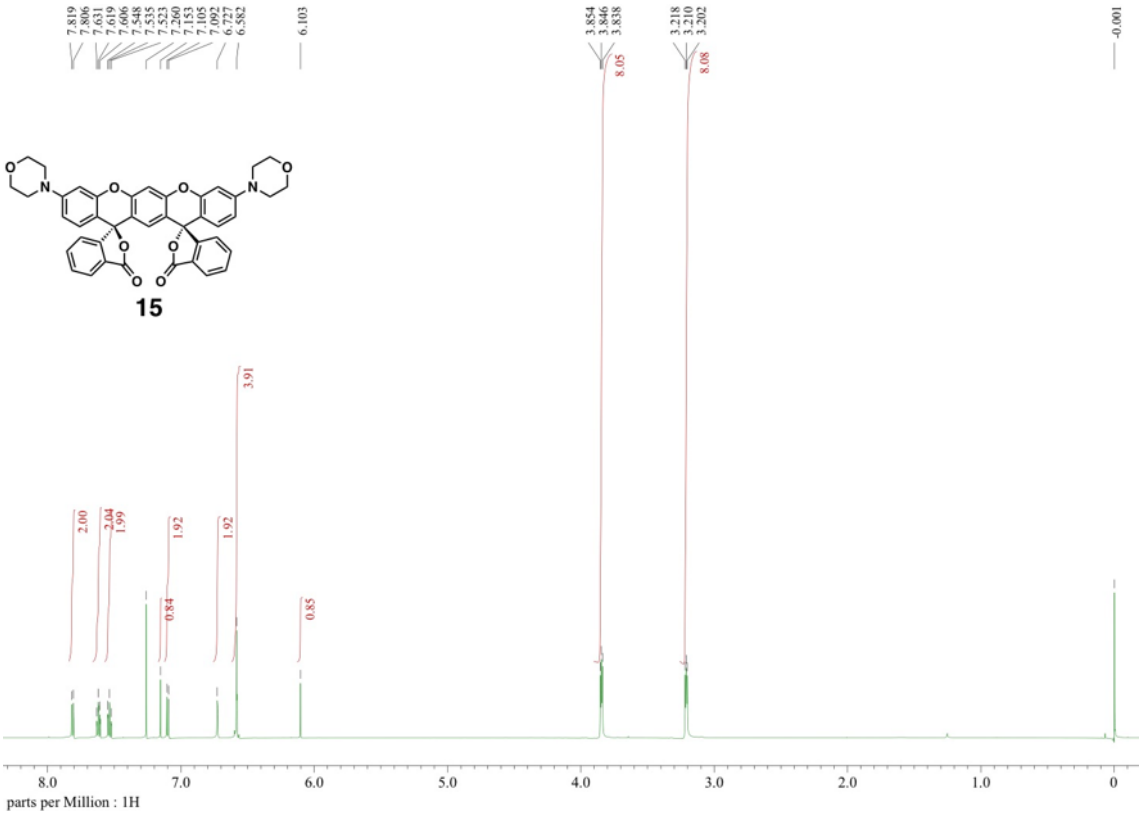
7.819
7.806
7.631
7.619
7.606
7.548
7.535
7.523
7.260
7.153
7.105
7.092
6.727
6.582
6.103
3.854
3.846
3.838
3.218
3.210
3.202
-0.001
8.05
8.08
3.91
2.00
2.04
1.99
1.92
1.92
0.84
0.85
8.0
7.0
6.0
5.0
4.0
3.0
2.0
1.0
0
parts per Million : 1H

15

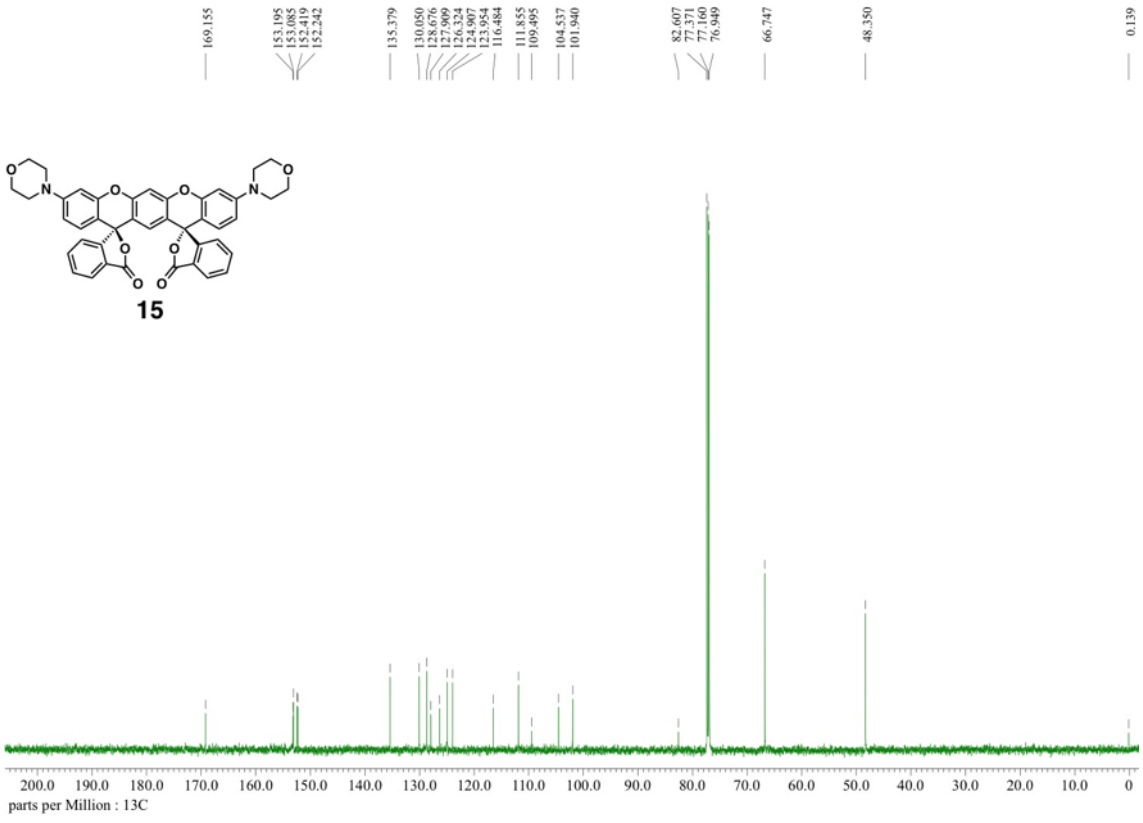
169.155
153.195
153.085
152.419
152.242
135.379
130.050
128.676
127.909
126.334
124.907
123.954
116.484
111.855
109.495
104.537
101.940
82.607
77.371
77.160
76.949
66.747
48.350
0.139
200.0
190.0
180.0
170.0
160.0
150.0
140.0
130.0
120.0
110.0
100.0
90.0
80.0
70.0
60.0
50.0
40.0
30.0
20.0
10.0
0
parts per Million : 13C

15

10. Cartesian Coordinates and Total Electron Energy

Compound **1** (S_0)

E (rCAM-B3LYP/6-31G(d,p)) = -2181.98629010 hartrees

Atom	Coordinates (Å) X	Y	Z	Atom	Coordinates (Å) X	Y	Z
C	-1.1992	-1.32043	-0.16457	C	8.99307	-1.69662	1.29178
C	-1.22273	0.07113	-0.28252	C	6.67821	-4.93723	-0.9046
C	-0.00206	0.73168	-0.35103	N	-7.02238	-2.68038	0.21401
C	1.21874	0.06998	-0.29772	C	-8.37498	-2.17044	0.36874
C	1.19525	-1.32147	-0.17878	C	-6.86915	-4.1253	0.18583
C	-0.0019	-2.01634	-0.10744	C	-6.58495	-4.7401	1.55481
C	2.52119	0.82679	-0.41197	C	-9.08592	-1.89575	-0.95467
C	3.69701	-0.09554	-0.23156	H	-0.00222	1.81233	-0.45114
C	3.5459	-1.47076	-0.11634	H	-0.00178	-3.09442	-0.01145
O	2.32043	-2.08175	-0.10656	H	5.17331	1.45456	-0.31823
C	5.009	0.38536	-0.22902	H	7.08922	-0.00232	-0.09855
C	6.10243	-0.44391	-0.11234	H	4.40335	-3.39131	0.06675
C	5.93796	-1.8448	0.00527	H	-4.40417	-3.38303	0.16905
C	4.62576	-2.3357	0.00228	H	-7.09108	0.00313	-0.0333
O	-2.32418	-2.07985	-0.08073	H	-5.175	1.46057	-0.24222
C	-3.54915	-1.4678	-0.07503	H	2.84927	5.32397	-0.38013
C	-3.69965	-0.09153	-0.17887	H	2.79431	5.52842	2.11908
C	-2.52582	0.82908	-0.37949	H	2.6079	3.51049	3.51887
C	-4.62791	-2.3307	0.06619	H	2.47178	1.2538	2.49319
C	-5.93938	-1.83795	0.08813	H	-2.43153	1.2641	2.52315
C	-6.10347	-0.43658	-0.02293	H	-2.54982	3.5238	3.54451
C	-5.0104	0.39174	-0.14936	H	-2.75573	5.53798	2.14204
O	2.59313	1.41886	-1.75337	H	-2.8492	5.32657	-0.35543
C	2.7032	2.77443	-1.71365	H	7.73943	-4.4571	0.91168
C	-2.56947	2.05198	0.51815	H	6.01121	-4.26513	1.04581
C	-2.68668	3.18465	-0.26231	H	8.98912	-3.02935	-0.40433
C	2.68611	3.18193	-0.2905	H	8.42038	-1.4259	-0.782
C	2.57971	2.04716	0.48846	H	10.0223	-1.3608	1.13563
C	2.76619	4.4532	0.26104	H	8.41623	-0.86113	1.69523
C	2.73495	4.55453	1.64489	H	9.0055	-2.48809	2.04633
C	2.62849	3.40755	2.43861	H	6.56972	-5.99863	-0.66346
C	2.55049	2.13981	1.87197	H	5.79417	-4.6196	-1.46214
C	-2.72583	2.77318	-1.68392	H	7.54449	-4.82675	-1.56283
O	-2.61737	1.41748	-1.72157	H	-8.94083	-2.91024	0.94372
C	-2.51896	2.14847	1.90077	H	-8.35519	-1.26929	0.98774
C	-2.58704	3.41786	2.46499	H	-7.793	-4.54726	-0.22214
C	-2.70458	4.5627	1.66976	H	-6.08278	-4.39227	-0.52573
C	-2.75714	4.45752	0.28683	H	-6.49408	-5.8275	1.47918
O	2.7997	3.45639	-2.69692	H	-5.6581	-4.34686	1.97881
O	-2.8369	3.45257	-2.66745	H	-7.39392	-4.51574	2.2557
N	7.02156	-2.68753	0.12453	H	10.1018	-1.53006	-0.77899
C	6.85518	-4.11055	0.36753	H	-8.54855	-1.14871	-1.5433
C	8.38555	-2.20382	-0.01448	H	-9.15367	-2.80691	-1.55556

11. References

1. Tanioka, M.; Kamino, S.; Muranaka, A.; Ooyama, Y.; Ota, H.; Shirasaki, Y.; Horigome, J.; Ueda, M.; Uchiyama, M.; Sawada, D.; Enomoto, S. *J. Am. Chem. Soc.* **2015**, *137*, 6436−6439.
2. Liu, Q. H.; Yan, X. L.; Guo, J. C.; Wang, D. H.; Li, L.; Yan, F. Y.; Chen, L. G.; *Spectrochim Acta Part A* **2009**, 73, 789–793.
3. Burla, M. C.; Caliandro, R.; Camalli, M.; Carrozzini, B.; Cascarano, G. L.; Giacovazzo, C.; Mallamo, M.; Mazzone, A.; Polidori, G.; Spagna, R. *J. Appl. Crystallogr.* **2012**, *45*, 357–361.
4. Sheldrick, G. M. *Acta Crystallogr., Sect. A: Found. Adv.* **2008**, *A64*, 112–122.
5. Farrugia, L. J. *J. Appl. Crystallogr.* **1997**, *30*, 565–566.
6. Spek, A. L. *J. Appl. Crystallogr.* **2003**, *36*, 7–13.
7. Gaussian 09, Revision D.01, Frisch, M. J.; Trucks, G. W.; Schlegel, H. B.; Scuseria, G. E.; Robb, M. A.; Cheeseman, J. R.; Scalmani, G.; Barone, V.; Mennucci, B.; Petersson, G. A.; Nakatsuji, H.; Caricato, M.; Li, X.; Hratchian, H. P.; Izmaylov, A. F.; Bloino, J.; Zheng, G.; Sonnenberg, J. L.; Hada, M.; Ehara, M.; Toyota, K.; Fukuda, R.; Hasegawa, J.; Ishida, M.; Nakajima, T.; Honda, Y.; Kitao, O.; Nakai, H.; Vreven, T.; Montgomery, J. A., Jr.; Peralta, J. E.; Ogliaro, F.; Bearpark, M.; Heyd, J. J.; Brothers, E.; Kudin, K. N.; Staroverov, V. N.; Kobayashi, R.; Normand, J.; Raghavachari, K.; Rendell, A.; Burant, J. C.; Iyengar, S. S.; Tomasi, J.; Cossi, M.; Rega, N.; Millam, M. J.; Klene, M.; Knox, J. E.; Cross, J. B.; Bakken, V.; Adamo, C.; Jaramillo, J.; Gomperts, R.; Stratmann, R. E.; Yazyev, O.; Austin, A. J.; Cammi, R.; Pomelli, C.; Ochterski, J. W.; Martin, R. L.; Morokuma, K.; Zakrzewski, V. G.; Voth, G. A.; Salvador, P.; Dannenberg, J. J.; Dapprich, S.; Daniels, A. D.; Farkas, Ö.; Foresman, J. B.; Ortiz, J. V.; Cioslowski, J.; Fox, D. J. Gaussian, Inc., Wallingford CT, 2009.
8. Yanai, T.; Tew, D. P.; Handy, N. C. *Chem. Phys. Lett.* **2004**, *393*, 51–57.